JPRS-UMS-89-004
29 DECEMBER 1989

FOREIGN BROADCAST INFORMATION SERVICE

JPRS Report

Science & Technology

USSR: Materials Science

Science & Technology
USSR: Materials Science

JPRS-UMS-89-004 *29 DECEMBER 1989*

CONTENTS

Miscellaneous

UDC 669.295.5:539.50:009.788

Relationship of Maximum Permissible Concentration of Hydrogen in Titanium Alloy to Strength Characteristic

18420195 Ordzhonikidze IZVESTIYA VYSSHIKH UCHEBNYKH ZAVEDENIY TSVETNAYA METALLURGIYA in Russian No 6, Feb 88 (Manuscript received 26 May 88) pp 124-125

[Article by V. D. Talalaev, B. A. Kolachev, Stupinskiy Affiliate, Moscow Institute of Aviation Technology]

[Text] To evaluate the safety of titanium alloys in use, we must know the permissible concentrations of hydrogen $C_{\text{per d op}}$. They are evaluated by the equation

$$C_{\text{доп}} = C_{\text{кр}}/n, \quad (1)$$

where C_{cr} is the critical hydrogen content, above which mechanical properties drop sharply, while n is the reserve factor, considering the importance of the structure, its usage conditions and manufacturing technology.[1, 2]

The critical concentration is estimated from the results of impact toughness testing of the product if subject only to impact loading, or the results of long-term tensile testing and fracture toughness if the structure must operate for long periods under static loadings.[1] However, at the present time, the possible variation of coefficient n as a function of the strength of the material in connection with the ascending diffusion of hydrogen in the stress field is not considered.

The tendency of titanium alloys toward second order hydrogen embrittlement increases with increasing strength, since the accumulation of hydrogen in the stress field is determined by the equation[3]

$$C^{\sigma}_{max} = C_0 \exp(\overline{V}_H \sigma_h/RT), \quad (2)$$

where C_0 is the mean concentration of hydrogen in the metal, V is mean value of $_H$ is the partial molar volume of hydrogen in the metal, σ_h is the hydrostatic pressure, R is the gas constant, T is the absolute temperature.

For α and β titanium alloys, the partial molar volume of hydrogen is equal to 2 and 4 cm^3/mol.[4] In α+β-titanium alloys, hydrogen is concentrated in the β phase, and therefore the effective partial molar volume for them is 4 cm^3/mol[4]. The maximum value of σ_h is approximately $3\sigma_T$ (where σ_T is the yield point); if σ_T is expressed in MPa, at room temperature equation (3) becomes: for α alloys $C^{\sigma}_{max}=C_0 \exp(2.5\cdot10^{-3}\sigma^T)$; for α+β- and β alloys $C^{\sigma}_{max}=C_0 \exp(5\cdot10^{-3}\sigma_T)$.

We present below the maximum possible concentrations of hydrogen in the zone of triaxial extension in advance of a crack tip with various levels of yield point:

σ_T, MPa	600	800	1000	1200	1400
C^{σ}_{max}/C_0 (where V is mean value of $_H$ = 2cm^3/mol)	4.5	7.4	12	20	33
C^{σ}_{max}/C_0 (where V is mean value of $_H$ = 4 cm^3/mol)	20	55	148	403	1096

Long-term tensile testing automatically considers redistribution of hydrogen at the crack tip, since the test system supports ascending diffusion of hydrogen. In these tests, the formation and propagation of a crack occur not at the average hydrogen content, but at the content of hydrogen accumulated as a result of ascending diffusion. For this reason, long-term tensile testing yields the hardest estimate of critical hydrogen concentration. Nevertheless, redistribution of hydrogen in a stress field must be considered even with this estimate of C_{cr}, since in a structure, in addition to the local ascending diffusion in the stress field of a crack, a field of residual and usage stresses may act strongly over distances comparable to the dimensions of the loaded elements of a structure. The redistribution of hydrogen resulting from long-acting stress fields is not as great as at the tip of a crack, since it is caused not by hydrostatic pressure $\sigma_h = 3\sigma_T$, but rather by the residual usage stresses, which are less than the yield point. However, it is in the hydrogen-rich zone that slow failure may start, at a hydrogen concentration which is greater than the average for the volume.

If we limit ourselves to a scheme of linear uniaxial extension, then in estimating the accumulation of hydrogen in the field of long-acting stresses in equation (2), σ_H should be replaced by the normal stress σ. On the assumption that residual stresses in structures should not exceed 0.75 times the yield point, equation (2) becomes

$C^{\sigma}_{max} = C_0 \exp(1.2\cdot10^{-3}\alpha_T)$ where V is mean value of $_H$ = 4 cm^3/mol and $C^{\sigma}_{max} = C_0 \exp(0.6\cdot10^{-3}\sigma_T)$ where V is mean value of $_{H\ -\ 2\ cm^3}$/mol. Then the ratio C^{σ}_{max}/C_0 in zones of extension at various levels of yield point and V is mean value of $_H$ = 4 cm^3/mol becomes:

σ_T, MPa	600	800	1000	1200	1400
C^{σ}_{max}/C_0	2	2.63.3	4.2	5.4	

Thus, the reserve factor in titanium structures should be greater, the higher the yield point.

Permissible Concentrations of Hydrogen in Titanium Alloys Considering Level of Residual Stresses

Alloy	State	$\sigma_{0.2}$, MPa	C_{cr}% (by mass)	$n = C^{\sigma}_{max}(over)C_0$	C_{sup}, % (by mass)
VT5L	annealed	630	0.014	1.46	0.01
OT4-1	annealed	530	0.005	1.37	0.004
OT4	annealed	660	0.010	1.49	0.007
VT5-1	annealed	730	0.015	1.55	0.01
VT20	annealed	890	0.020	1.70	0.012
VT6	hardened	860	0.045	2.81	0.016
VT6	hardened + aged	1030	0.015	3.44	0.005
VT3-1	annealed	900	0.03	2.94	0.01
VT14	annealed	920	0.05	3.01	0.017
VT16	hardened + aged	980	0.05	3.24	0.015
VT22	hardened + aged	1080	0.05	3.67	0.014
VT30	hardened	600	0.10	2.05	0.05

The table presents permissible hydrogen concentrations in titanium alloyos considering their yield point and C_{cr}, taken from[1, 2] based on the results of long-term tensile testing. For α and pseudo α- alloys, we assume V is mean value of $_H$ = 2 cm^3/mol, for α+β and β alloys—4 cm^3/mol.

The safe permissible concentrations of hydrogen in structures should be somewhat less than those presented, since, in addition to the strength level, we should also consider fluctuations in the chemical composition of the alloy, inaccuracies in determining the hydrogen concentration and the mechanical properties, possible deviations from recommended technology of manufacture of intermediate products and structures. We note in conclusion that the data presented in the table are correct for a bar about 20 mm in diameter, and when computing hydrogen tolerances for actual structures should be adjusted considering the geometry and dimensions of the structures.[2]

Bibliography

1. S. A. Vigdorchik, B. V. Kolachev, Protsessy obrabotki legkikh i zharoprochnykh splavov [Processes of Working Light and Heat- Resistant Alloys], Moscow, Nauka Press, 1981, pp 71-78.

2. A. V. Malkov, B. A. Kolachev, Metallovedeniye legkikh splavov [Physical Metallurgy of Light Alloys], Moscow, All-Union Institute of Light Alloys, 1985, pp 118-125.

3. B. A. Kolachev, Vodorodnaya khrupkost metallov [Hydrogen Embrittlement of Metals], Moscow, Metallurgiya Press, 1985.

4. A. V. Fishgoit, B. A. Kolachev, Izv. vuzov. Tsvetnaya metallurgiya, 1985, No. 1., p 135.

UDC 621.9.048.4

Broaching of Very Deep Small-Diameter Holes by Electroerosion

18420146A Kishinev ELEKTRONNAYA OBRABOTKA MATERIALOV in Russian No 1, Jan-Feb 89 (manuscript received 28 Dec 87) pp 5-8

[Article by E. T. Abdukarimov and S. Ya. Saidinov, Tashkent]

[Text] Electroerosion machining (EEM) has a special place among the various metal working methods. It is used when other methods are ineffective, for example in machining of very hard and ductile materials. However, the possibilities of EEM are also limited. One of the most difficult tasks for EEM, as for almost all methods of machining, is the broaching of deep holes. This task is particularly difficult in the case of the machining of small-diameter holes, which is due to the difficulties with removal of machining products from the hole. Also, in EEM there is a lateral-erosion effect, which becomes important in the case of deep holes. If these shortcomings are eliminated, EEM can be used to make holes of practically any depth and diameter.[1-4]

The present paper reports experimental data obtained in the development of methods for deep broaching of holes in electrically conductive materials, with hole diameters ranging from 0.5 to 4.0 mm and depth-to-diameter ratios ranging from 100 to 200 and more, depending on the hole diameter and part material. These data are needed to determine the capabilities of this new method and of its areas of application in order to use it on a broad scale in the national economy. These results were obtained chiefly owing to the design features of the electrode tool. The new method is protected by an USSR authorship certificate[5] and is patented abroad.[6]

Copper, brass, stainless steel 12Kh18N10T, polycrystalline tungsten, titanium, and heat-resistant alloy ZhS6-U were selected as experimental materials. A tungsten wire of type VA and VRN-1 (GOST 19671-74) was used as the electrode tool (direct polarity was used in the studies). An RC generator was used as a source of current pulses. Its performance parameters were as follows: Mean working current not exceeding 10 A, maximum pulse current not exceeding 800 A, pulse repetition frequency less than 1 kHz, current-pulse duration not more than 100 microseconds. The pulse energy was varied between 0.001 and 1.0 J. A control system provided a stable interelectrode gap and automatic continuous feed of the electrode tool into the hole during the entire EEM process. Ordinary water with a specific resistance of about 1000 ohm-meters was used as the working liquid.

Figure 1 shows the experimentally determined variation of the rate of broaching of holes of various diameters with their depth for the materials listed above. It is clear that super-hard and high-melting materials are more resistant to erosion by electrical discharge than the metals with lower melting temperatures. For small depths the rate of erosion is somewhat higher than average because the conditions of evacuation of molten metal from the interelectrode gap are better than they are at greater depths. In spite of the fact that the conditions for removal of the machining products and for restoration of the interelectrode gap for subsequent electrical discharges become less favorable as the electrode tool penetrates into the part, the rate of broaching stabilizes. The rate of erosion of the electrode tool and of the part varies with the changing energy and duration of the pulse when holes are broached with an identical electrode tool (Figure 2). At the same time, the hole diameter also changes slightly. Because our method permits very deep holes to be broached, the relative consumption of the electrode tool is reported in percent (the ratio of the length l_k of the electrode that is consumed to the length l_a of the hole broached). The electrode consumption varies greatly with the thermophysical properties of the part. Thus, in the case of copper the relative electrode consumption is 20-50 percent, while in the case of tungsten it is 100-200 percent. If the relative consumption is expressed in terms of volume, it decreases by a factor of 2.5-3.0, because the hole diameter is considerably larger than the electrode diameter. For example, an electrode with a diameter of 1.0 mm makes a hole with a

Figure 1. Variation of the Rate of Broaching of Holes With Depth for (a)—copper, (b)—brass, (c)—stainless steel 12Kh18N10T, (d)—alloy ZhS6-U (upper curve) and titanium, (e)—tungsten.

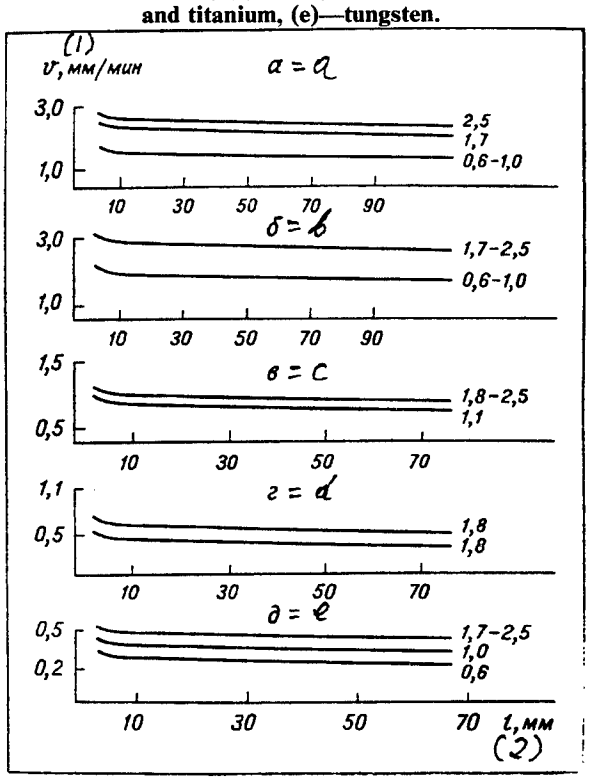

The numerals denote the hole diameter in mm.
Key: (1)—V, mm/min; (2)—l, mm

Figure 2. Variation of the Rate of Broaching and Electrode-Tool Wear With No-Load Voltage U_{nl} and Condenser Capacitance C When Broaching 2.0-mm Dia. Holes in Copper

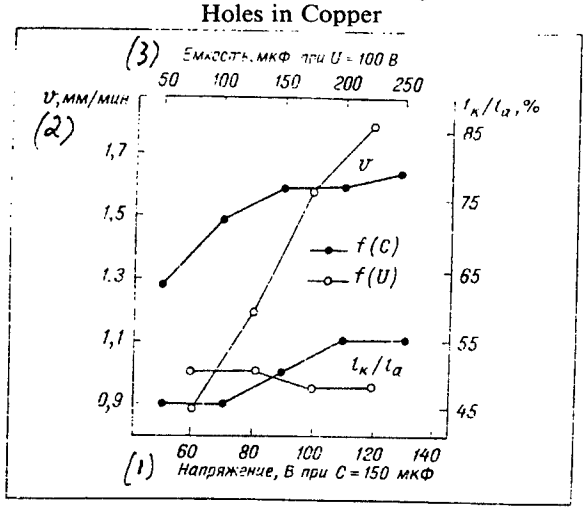

Key: (1)—voltage, V at C=150 μΦ; (2)—V, mm/min; (3)—capacitance, μΦ at U=100 V

diameter of at least 1.6 mm. The electrode consumption is partly due to the inductance of the capacitances used and to the difference between the wave resistance of the charging and discharging circuits.

Cleanliness of the hole is an important characteristic. It varies considerably with the pulse energy and the dielectric medium.[7-9] Studies of the surface by means of a profilograph-profilometer (type A1, model 252) showed that when the pulse energy is 0.4-1.0 J, the mean arithmetic deviation R_a of the surface roughness (profil) varies between 6 and 15 microns. R_a does not exceed 3 microns when the pulse energy is less than 0.1 J.

The analysis of the profilograms and of the table data shows differences between the surfaces produced in ordinary and distilled water with the same parameters of the charging circuit (Figure 3). This can be attributed to the higher breakdown voltage in distilled water compared to the discharge in ordinary water. Also, it is possible that the presence of impurities promotes electrochemical processes in ordinary water. Photographs of the hole surface, together with the profoilograms (Figure 3), give a complete picture of the unevennesses that result from the intersection of pit boundaries and the sticking of the erosion products to the surface.

Variation of Surface Roughness of a Hole With Pulse Energy and Dielectric Medium (U=100 V)

	R_a, μm	
C, μΦ	ordinary water	distilled water
	copper	
100	4.4	8.1
150	4.6	8.4

Figure 3. Profilograms of Hole Surfaces

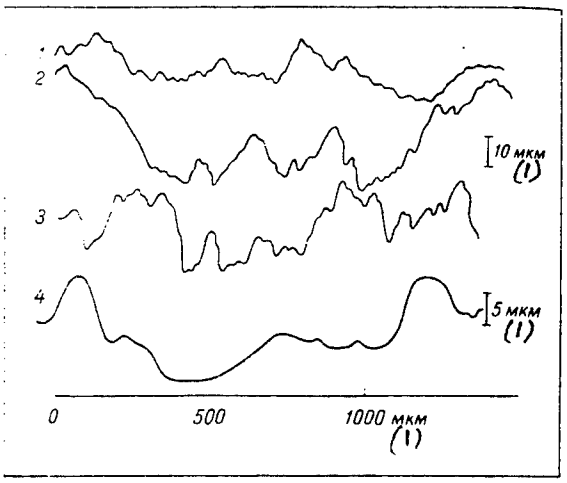

Modes and conditions of machining: 1-3—copper, 4—stainless steel. U=100 V (1-4). C, : 1 and 3—100; 2—250; 4—170. 1, 2, 4—ordinary water; 3—distilled water

Key: (1)—μm

200	5.4	9
245	6.9	10
stainless steel		
100	4.6	—
150	—	—
200	5.3	—
245	5.5	—

It is known that EEM produces changes in the surface layer.[1, 4, 10]. Owing to the rapid cooling by the working fluid, a surface layer with an altered structure is produced under the pressure of gases, vapors, liquid, and metal. Measurements of microhardness of the surface layer in copper and steel after EEM showed that this layer is nonuniform with regard to hardness (Figure 5). Apparently, the shape of the microhardness curves can be attributed to annealing of the surface layer of copper, which leads to a sharp decrease in microhardness (the increased microhardness of the layer near the surface is attributed to penetration of the electrode material into the body of the part,[11] and to quenching of the surface layer of steel.

The erosion products are finely dispersed particles of mainly spherical shape. Their size varies from hundreds of Angstroms to tens of microns. Irregularly shaped particles with fused edges are encountered in the coarse fraction. The smallest fraction of the particles is surrounded by branch-like conglomerates, which apparently form as a result of condensation of metal vapors and colloidal suspension.

As our studies showed, the main advantages of the new method of electroerosion broaching of holes are the fact

Figure 5. Variation of Microhardness of Surface Layer of Copper (a, b) and Stainless Steel 12Kh18N10T (c, d)

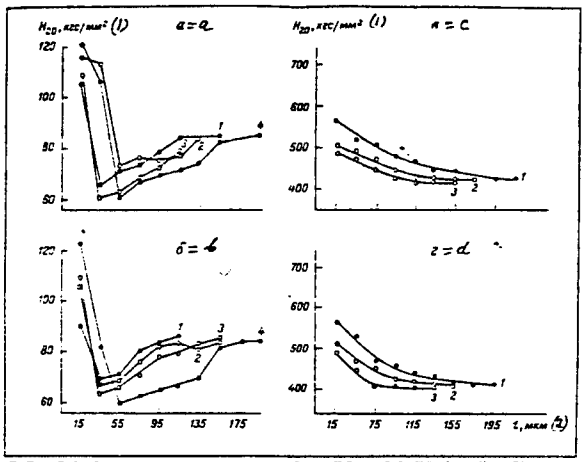

Machining parameters: a, b—U=100 V (1-4); C, : 1—100; 2—150; 3—200; 4—245. c, d: U, V: 1—120, 2—100, 3—60. C, : 1—245; 2—150; 3—100. Dielectric medium: a, c—ordinary water, b, d—istilled water.
Key: (1) H_{20}, kgf/mm^2; (2) *l*, μm

that the rate of erosion is practically independent of the depth and the precision of the holes. This is achieved by efficient removal of the erosion products from the interelectrode gap and elimination of lateral erosion over the entire length of the electrode tool.

This method will broaden the range of applications of the electroerosion machining of metals. It may find use in machining of holes in lubrication, cooling, and fuel-supply systems in various engines and in the creation of through and blind holes in cutting tools, dies, etc.

Bibliography

1. B. N. Zolotykh, "Basic Problems of the Qualitative Theory of Electrosparking in a Liquid Dielectric Medium" in "Problemy elektricheskoy obrabotki materialov" [Problems of the Electric Machining of Materials], Moscow, 1962, pp 5-44.

2. B. G. Gutkin, A. L. Livshits, "Electric-Pulse Machining of Metals" in "Elektrorazryadnaya obrabotka materialov" [Electric-Discharge Machining of Materials], Leningrad, 1971, pp 121-196.

3. e. M. Levinson, "Otverstiya malykh razmerov" [Small-Diameter Holes], Leningrad, 1977, pp 54-127.

4. B. R. Lazarenko, N. I. Lazarenko, "Elektroiskrovaya obrabotka metallov" [Electrosparking of Metals], Moscow, 1950.

5. USSR Authorship Certificate No. 1407711. Int. Class V 23 N 1/00, 9/14. "Method for Electroerosion Machining of Deep Holes," E. T. Abdukarimov. Published 7 Jul 88. Bull. No 25.

6. French Patent No 84 16809 (2 572 665). Int. Class V 23 N 7/22, 9/14. Published 23 Jan 87.

7. B. N. Zolotykh, "Fizicheskiye osnovy elektrofizicheskikh i elektrokhimicheskikh metodov obrabotki" [Physical Principles of Electrophysical and Electrochemical Machining Methods], Part 1, Moscow, 1975, pp 3-81.

8. K. K. Namitkov, "Elektroerozionnyye yavleniya" [Electroerosion Phenomena], Moscow, 1978.

9. N. B. Stavitskaya, B. I. Stavitskiy, "Study of the Shapes and Sizes of Erosion Pits Produced in Various Materials by Spark Discharge," ELEKTRONNAYA OBRABOTKA MATERIALOV, No 1, 1980, pp 9-13.

10. B. A. Artamonov, Yu. S. Volkov, V. I. Drozhalova, et al., "Elektrofizicheskiye i elektrokhimicheskiye metody obrabotki materialov" [Electrophysical and Electrochemical Methods of Processing Materials],Vol 1, Moscow, 1983, pp 4-95.

11. N. K. Foteyev, A. A. Kapyrin, "Transfer of Electrode-Tool Material to the Part Surface During Dimensional Electroerosion Machining," ELEKTRONNAYA OBRABOTKA MATERIALOV, No 2, 1986, pp 23-25.

UDC 532.536:621.9.048.4

Friction, Wear of Coatings Obtained by Electric-Spark Surface Hardening of AL-25 Alloy With High-Melting Compounds

18420146B Kishinev ELEKTRONNAYA OBRABOTKA MATERIALOV in Russian No 1, Jan-Feb 89 (manuscript received 6 May 87) pp 17-20

[Article by A. P. Abramchuk, G. A. Bovkun, V. V. Mikhaylov, and Yu. G. Tkachenko, Kishinev]

[Text] High corrosion resistance, satisfactory mechanical strength, and other properties make aluminum alloys very attractive for use in various mechanisms and structures as a replacement for traditional materials such as cast iron and steel. However, their use is limited by their insufficient wear resistance.

Strengthening of aluminum alloys by plasma and gas-plasma coating[1] or metallizing[2] entails certain difficulties and suffers from a number of shortcomings. Coatings on aluminum alloys obtained by these methods are porous and nonuniform and exhibit poor adhesion to the substrate.

Owing to the negligible heating and the absence of strain in the substrate, a high strength of bonding with the substrate, as well as the possibility of local strengthening using a broad range of coating materials, electric-spark strengthening with powder materials offers a number of process advantages.[3, 4] This method appears to be suitable for strengthening of aluminum and its alloys.[5] This is quite important because aluminum cannot be strengthened with compact electrodes.

It is known that metal-like and nonmetallic high-melting compounds, particularly boron and silicon carbides, have been traditionally used in production of coatings by plasma deposition.[6, 7]

This paper reports on a study of the phase composition, structure, microhardness, and friction characteristics of layers produced on aluminum alloy Al-25 by strengthening it with nonmetallic high-melting compounds AlN, Si_3N_4, SiC, B_4C and metal-like compounds TiC, ZrN, TiN, and TiB_2 by electric-spark strengthening with powder mixtures. The strengthening was carried out with an EFI-46A unit equipped with a device for feeding of powders to the interelectrode gap. The discharge-energy reserve was varied between 0.3 and 6 J. The powder particle size was 16-120 microns.

To lower the roughness of strengthened surfaces, the coatings were subjected to surface plastic strain with a 5-mm diameter steel ball. The friction and wear tests were carried out by subjecting specimens in the form of 16-mm dia. by 8-mm dia. by 15-mm bushings to end friction with an average relative slip rate of 0.01 m/s and contact zone pressure of 1-2 MPa. Specimens with like coatings or cast-iron (SCh 12-28) specimens were used as the abradant. The wear kinetics, and in the case of highly wear-resistant coatings, the variation of the friction coefficient with contact zone pressure, were studied in the course of the tests. The wear was determined by measuring the height of the specimens before and after testing with an accuracy of up to 1 micron with a IKV vertical optimeter. A PMT-3 hardness meter with an indentor load of 0.5 N (the indentor load was 0.2 N for measurement of the microhardness of the aluminum substrate) was used for measuring the microhardness of the coatings.

A DRON-3 diffractometer in filtered copper K-radiation was used to study the phase composition of hardened layers. The results are shown in the table. The analysis of the data in the table should be carried out based on the mechanisms of the chemical reaction of high-melting compounds with molten aluminum and the specifics of the effect of the spark discharge on the substrate and on the hardening powder mixture during electric-spark alloying.

Phase Composition, Thickness, and Hardness of Coatings on AL-25 Alloy

Powdered material	Nature of reaction with molten aluminum*	Phase composition	Thickness, μm	Microhardness, GPa
TiC	Does not react up to 1100 deg C; when T exceeds 1400 deg C, Al_4C_3 may form, and it decomposes in contact with molten aluminum.	TiAl, $TiAl_3$, Al_4	85	5.7
TiB_2	Does not react up to 1200 deg C; solid solution of aluminum in titanium diboride may form above 1250 deg C	TiAl, $TiAl_3$, AlB_{12}, Ti	75	6.0
TiN	Reacts above 1000 deg C with formation of $TiAl_3$ and AlN	TiAl, $TiAl_3$, AlN, Ti	75	4.5
ZrN	Reacts with formation of AlN and solid solution of aluminum in Zr	Zr_2Al, Zr_3Al_2, Zr_3Al, AlN	65	5.5
AlN	Does not react	AlN, Al	80	6.5
Si_3N_4	No information	AlN, Si	60	3.8
SiC	same as above	Al_4C_3, Si	65	4.0
B_4C	Reacts with formation of AlB_2, AlB_{12}, and Al_4C_3	Al_4C_3, AlB_{12}, AlB_2	60	6.5

*Data taken from[9]

It is known that hardening with powder mixtures has a greater effect on the substrate than hardening with compact electrodes. In the case of hardening with compact electrodes, it is almost always possible to fix the anode-electrode phases in the surface layer formed on the substrate,[8] whereas in the case of hardening with powder mixtures the mixture components undergo thermal dissociation, and the phase composition of the coatings is due to the directed transfer of dissociation products to the substrate and by their chemical reaction with the substrate materials. As a result, when an aluminum alloy is hardened with metal-like compounds, the hardened layer contains intermetallic compounds and compounds of aluminum with carbon, boron, and nitrogen, and only the latter are found when aluminum is hardened with high-melting nonmetallic compounds.

Metallographic studies showed that a 60-80 micron layer forms on analuminum surface after electric-spark hardening with powdered materials.

The coating hardness is determined by the hardness of the products of the reaction between aluminum and the powder mixtures, and it is maximum when the coating contains the AlB_{12}phase.

Figure 2 shows kinetic curves of the wear rate for coatings on an aluminum substrate. Comparison of the data from Figure 2 with those in the table shows that there is no clear relationship between the hardness and the wear-resistance of the coatings. Coatings containing the AlB_{12} phase show the highest wear resistance. Coatings produced by hardening of the aluminum alloy with

metal-like and nonmetallic nitrides show a satisfactory wear resistance. The lowest wear resistance was observed in coatings containing the carbide Al_4C_3; that is, the hardening effect of the phases decreases in the order AlB_{12}, AlN, Al_4C_3. One can also see that the wear resistance of coatings hardened with the powders of metal-like compounds changes with time in a similar manner, that it depends chiefly on the nature of the hardening phases (AlB_{12}, AlN, Al_4C_3), and that it is practically independent of the nature of the intermetallides in the coating. However, when the coatings obtained by hardening of the aluminum alloy with high-melting nonmetallic compounds do not contain intermetallides, their service life is short, and they begin to wear catastrophically after 3-5 hours of testing and show areas of unhardened substrate. Thus, the intermetallides in the coatings are responsible for the strength of holding the hardening phases of aluminum in the coating and for the bonding strength between the coatings and the substrate.

Figure 2. Kinetics of Change of Wear Rate of Like Coatings Obtained by Electric-Spark Hardening of the Aluminum Alloy With High-Melting Compounds

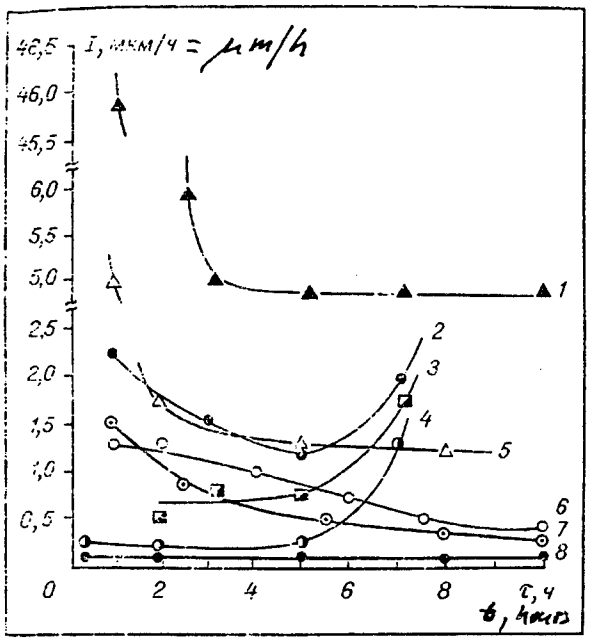

1—non-hardened alloy AL-25; 2—SiC; 3—Si_3N_4; 4—B_4C; 5—TiC; 6—TiN; 7—AlN; 8—TiB_2

Figure 3 shows the variation of the friction coefficient of the same kind of coatings on the aluminum alloy with the contact zone pressure. The coatings were tested for 45 minutes at each load. This time is sufficient for stabilization of the friction coefficient and formation of the surface relief characteristic for the given test conditions. The data in the table and in figures 2 and 3 show that electric-spark hardening with powders of high-melting compounds is capable of increasing the surface hardness of the AL-25 alloy by a factor of 2 to 3, lowering the surface friction coefficient by a factor of 2 to 3, and lowering the wear rate by a factor of 3 to 10, and more, in tests involving sliding friction in air. This shows that electric-spark hardening of aluminum and its alloys is a promising method. Also, it can be concluded on the basis of the present study that widely available powders of compounds that form AlB_{12} phases and Me_xAl_y intermetallides by reaction with molten aluminum can be used for hardening.

Figure 3. Variation of Friction Coefficient of Like Coatings with Contact Zone Pressure for Coatings Obtained by Electric-Spark Hardening of the Aluminum Alloy With High-Melting Compounds

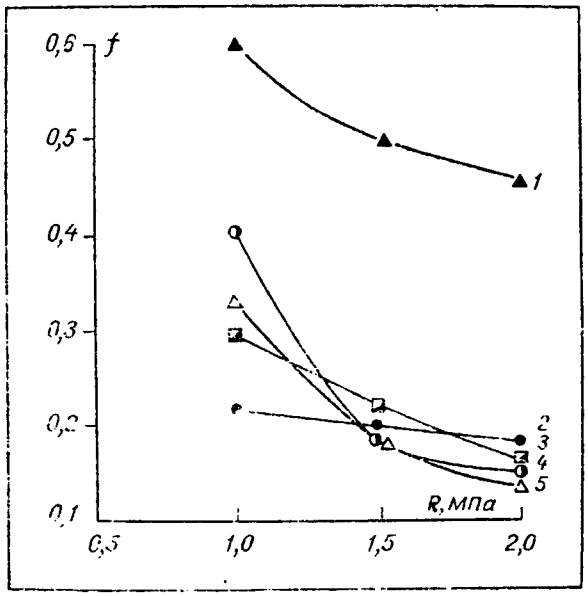

1—non-hardened alloy AL-25; 2—AlN; 3—TiN; 4—ZrN; 5—Si_3N_4

Bibliography

1. R. C. Tucker, "The Utilization of Plasma-deposited Coatings on Aluminum," SAE Preprint No. 760230.

2. T. Takahasi, "Treatment of Aluminum Surface by Metallization," ARUMINIUMU [Aluminum], No 487, 1971, pp 41-47.

3. A. Ye. Gitlevich, V. V. Mikhaylov, N. Ya. Tsarkanskiy, and V. M. Revutskiy, "Elektroiskrovoye legirovaniye metallicheskikh poverkhnostei" [Electric-Spark Alloying of Metal Surfaces], Kishinev, 1985.

4. USSR Authorship Certificate No. 1151403, Int. Class V23N 9/100, "Method of Application of Coatings and Apparatus for Carrying It Out," V. V. Mikhaylov, A. Ye. Gitlevich, V. M. Revutskiy and A. P. Abramchuk. Published 23 Apr 85, Bull. No 15.

5. V. V. Mikhaylov, A. P. Abramchuk A. P., "Features of Electric-Spark Alloying of Aluminum and Its Alloys," ELEKTRONNAYA OBRABOTKA MATERIALOV, No 2, 1986, pp 36-41.

UDC 621.793.734

Increasing the Stability of Mechanized Electric-Spark Alloying

18420146C Kishinev ELEKTRONNAYA OBRABOTKA MATERIALOV in Russian No 1, Jan-Feb 89 (manuscript received 15 Apr 86) pp 64-67

[Article by Yu. G. Noskov and V. P. Kulakov, Leningrad]

[Abstract] Causes of the disturbance of the stability of the mechanized electric-spark alloying (ESA) process are examined. Deficiencies of the sources of current to the vibrator coil and of the automatic regulators employing known ESA process parameters as input signals are demonstrated. A special source of stabilized current to the electrodynamic vibrator coil and a servo-system based on the size of the interelectrode gap with a photodiode sensor are proposed. The use of these devices in mechanized ESA units significantly increases the stability of the application of coatings and the principal performance figures of the process. References 5, figures 6.

UDC 621.9.047.7

Features of the Electrochemical Machineability of Maraging Steel 02N18K9M5T (EP-637)

18420146D Kishinev ELEKTRONNAYA OBRABOTKA MATERIALOV in Russian No 1, Jan-Feb 89 (manuscript received 19 May 86, after revision 19 May 87) pp 68-70

[Article by N. A. Amirkhanova, N. Z. Guinayev, A. F. Zorikhin, S. N. Sharipova, and L. P. Sharipova, Ufa]

[Abstract] Kinetic relationships of the rapid dissolution of steel 02N18K9M5T in a special electrochemical apparatus simulating a real electrochemical machining process were studied. It was shown that addition of sodium citrate to the sodium nitrate solution results in a considerable reduction of the height of the microunevennesses and maintains a high selectivity, thus ensuring high-precision machining. Tables 2, figures 3, references 8.

UDC 621.9.048

A Possible Way of Increasing the Precision of Electric-Spark Machining of Cavities With the Use of the Orbital Motion of the Electrode

18420146E Kishinev ELEKTRONNAYA OBRABOTAK MATERIALOV in Russian No l, Jan-Feb 89 (manuscript received 7 Jul 86) pp 71-73

[Article by B. A. Eyzner, Minsk]

[Abstract] A possible way of increasing the precision of electroerosion machining of a cavity with the use of orbital motion based on adaptive control of the frequency of the repetition of pulsed discharges is discussed. References 2, figures 4.

UDC 621.762.621.9.048.4

Preparation of Electrode Tools for Electroerosion Machining of Hard-Alloy Cutting Tools

18420146F Kishinev ELEKTRONNAYA OBRABOTKA MATERIALOV in Russian No 1, Jan-Feb 89 (manuscript received 1 Oct 86) pp 73-74

[Article by T. A. Zatsepina, Moscow]

[Abstract] An auxiliary master cutting tool is introduced in shaping operations in order to increase the precision and lower the labor content of the electroerosion machining of complex shapes, particularly lathe tools. The simplicity of making the master tool and the increase in the precision of the machining of special shapes as a result of installing the master tool and the part being machined on the same device increases the productivity of the machining of special surface shapes by a factor of 1.3. Reference 1, figures 4.

UDC 621.921.34:621.318.12

Bipolar Electro-Diamond Polishing in the Machining of Magnetically Hard Alloys

18420146G Kishinev ELEKTRONNAYA OBRABOTKA MATERIALOV in Russian No 1, Jan-Feb 89 (manuscript received 29 Dec 86) pp 74-77

[Article by A. M. Dolgikh, Saratov]

[Abstract] Principles of the selection of the process of single-pass bipolar electro-diamond grinding simultaneously with finishing as a promising approach to the development and improvement of electric machining are discussed. Analytical derivation of some special features of the kinematics of the abrasive grains of the finishing part of the tool is presented. The design of a new

electrode-tool for bipolar electro-diamond grinding is described. The principle processes occurring in the contact zone and their qualitative analysis are shown. It was found that practical use of diamond-abrasive grinding in an electric field with a bipolar electrode blank is a way to rapidly develop the technology of mechanical machining of hard-to-machine materials. References 3, figures 4.

UDC 621.9.048

Comparative Analysis of Process Productivity Increase in the High-Frequency Electroerosion Broaching of Small-Diameter Holes

18420146H Kishinev ELEKTRONNAYA OBRABOTKA MATERIALOV in Russian No 1, Jan-Feb 89 (manuscript received 4 Jan 87, after revision 16 Sep 87) pp 77-81

[Article by A. F. Boyko, Belgorod]

[Abstract] Calculations are reported that show the possibility of increasing the productivity of the electroerosion broaching of small holes by a factor of 1.68 to 1.75 by using a high-frequency transistor pulse generator instead of the relaxation-type RC-generator. Series production of precision model 04EP-10M machine tools has been developed and mastered. Their use confirmed the effectiveness of the use of a high-frequency transistor generator of short pulses as a source of the process current. The machine tools are used for broaching 0.015-0.5 mm dia. holes. About 200 units have been manufactured and placed in service. An industrial machine-tool unit received a gold medal at the Moscow Exhibition of the Achievements of the National Economy of the USSR. References 8, figures 5.

UDC 539.211:537.533

Electron-Probe Diagnosis of Ion Methods of Forming Film Structures

18420146I Kishinev ELEKTRONNAYA OBRABOTKA MATERIALOV in Russian No 1, Jan-Feb 89 (manuscript received 4 Jan 87) pp 81-84

[Article by N. Ye. Levchuk, V. Ya. Shiripov, and A. P. Dostanko, Minsk]

[Abstract] Ion beams are being used with increasing frequency in the technology of microelectronics products in the forming of complexmicroheterogeneous structures. Knowledge and monitoring of the processes occurring in the interaction of charged particles with a microheterogeneous structure is the most important requirement for the reproducibility and stable operation of the structure produced in this manner. The existing diagnostic methods permit recording of the results of an already completed process, and they do not provide information regarding process dynamics. A method is proposed that makes it possible to note the changes in the structure and composition of test specimens at any stage of their reaction with ions. It is shown that the method can be used in the study of the kinetics of the processes occuring during the action of ions on pure multicomponent and microheterogeneous structures. References 13, figures 4.

UDC 621.9.048:621.762

Optimization of the Chemical Composition of a Powder-Based Electrode-Tool by the Experiment Planning Method

18420146J Kishinev ELEKTRONNAYA OBRABOTKA MATERIALOV in Russian No 1, Jan-Feb 89 (manuscript received 5 Oct 87) pp 85-86

[Article by V. P. Nestorenko, F. P. Sanin, A. N. Kvasha, V. I. Zhura, S. A. Bozhko, and P. N. Mironenko, Dnepropetrovsk]

[Abstract] The effect of the nickel and manganese content in a copper base on the wear and productivity of electrode-tools for electric-spark dimensional machining was studied. The method of mathematical experiment planning (the method of Sheffe simplex grids) was used. After processing of experimental data with an ES-1050 computer, diagrams of the variation of the properties studied was constructed. The diagrams make it possible to establish the ranges of maximum productivity and minimum wear. References 5, table 1, figure 1.

UDC 621.9.047:002.001.18

Determination of Trends in the Industrial Use of Electrochemical Machining of Metals Based on Analysis of Information Flows

18420146k Kishinev ELEKTRONNAYA OBRABOTKA MATERIALOV in Russian No 1, Jan-Feb 89 (manuscript received 22 Apr 88) pp 87-89

[Article by M. N. Lemberskiy and G. N. Zaydman, Kishinev]

[Abstract] It was shown by analyzing information flows that during recent years there has been a trend toward increasing the industrial use of the electrochemical dimensional machining of metals. Differentiation of information flows has made it possible to establish that electrochemical machining is predominantly used in shaping operations. Electrochemical machining is used least in finishing and decorative operations. References 6, figures 5.

UDC 621.791:669

Thermophysical Factors of Structure Formation in Electron-Beam Hardening

18420182 Novosibirsk IZVESTIYA SIBIRSKOGO OTDELENIYA AKADEMII NAUK SSSR: SERIYA TEKHNICHESKIKH NAUK in Russian No 6, Dec 88 (manuscript received 1 Dec 87) pp 49-53

[Article by M. V. Radchenko, Altay Polytechnical Institute imeni I. I. Polzunov, Barnaul]

[Text] When alloys are cooled rapidly from the liquid state in a vacuum, significant changes occur in the structure of the metal, leading to an increase in its strength.[1-4] The formation of such a structure is a rather complex, rapidly occurring process, determined by a number of factors. Its study involves the investigation of thermophysical, hydrodynamic and other processes. One of the most effective means of investigation of rapidly occurring processes is mathematical modelling.[5] However, in order to compose an accurate mathematical model, it is necessary to have a set of statistical data on the values of the temperature gradients, cooling rates, true crystallization rates of individual microscopic volumes as well as of the entire metal bath, plus information on the type of, and presence of defects in, the structure, the dimensions of its components and structural and chemical heterogeneity. The search for and study of these parameters are governed by the correctness of the physical concepts of the process of accelerated crystallization of alloys.

This article presents the results of studies of the process of structure formation during electron-beam hardening in a vacuum with self-hardening from the liquid state at supercritical cooling rates using the example of a heterophase structural alloy.

The major thermophysical factors of structure formation during electron-beam hardening are melting of the metal, accompanied by its evaporation in the vacuum, refining of the liquid phase, its cooling at supercritical speeds, rapid crystallization and the pressure of the vapor-gas flow. Let us study these specifics of structure formation in sequence.

Evaporation of Metal

As we know, the transition from melting conditions, described by thermal-conductivity equations, to evaporation conditions depends basically on the concentration of heat in the source. With a power density at the spot heated by an electron beam on the order of $q = 10^4$—$10^5 W \cdot cm^{-2}$, which is characteristic for electron-beam hardening, the process of evaporation of the metal becomes significant. One result of this may be selective evaporation of alloying elements and a changing of the chemical composition of a melted multicomponent alloy, thus changing its physical and mechanical properties.

The rate of evaporation of a substance in a vacuum can be determined based on the solution of the Langmuir equation[6]:

$$V_и = 133P\sqrt{\frac{M}{2\pi RT_и}}, \qquad (1)$$

where P is the vapor pressure at temperature T_i, N/m^2; M is the molecular mass of the metal; R is the universal gas constant, 8.31 J/(K·mol); T_i is the evaporation temperature, K. For the major alloying elements contained in structural steel (Cr, Ti, Ni, Mo, W, etc.), the value of P where $T = T_i$ is on the order of 50-120 mmHg.[7, 8]

In calculations, considering the monoatomic nature of metal vapor, the value of M was taken to be equal to the atomic mass of the element. The temperature of the liquid metal bath surface was assumed to be equal to the boiling point. A numerical estimate of the mass velocity of evaporation for each of the elements yields the following values:

Element	Fe	Cr	Ti	Ni	Mo	Mn	Mg
M	55.847	51.996	47.90	58.71	95.94	58.938	24.305
V_i, $g \cdot cm^{-2} \cdot s^{-1}$	0.5487	0.5477	0.4478	0.5486	0.5477	0.6324	0.5470

Considering our assumptions, the numerical estimate shows that the rate of evaporation of most alloying elements in the process of electron-beam hardening in a vacuum is approximately the same, and we can therefore determine the mean mass rate of evaporation of the metal. This leads us to the conclusion that the conditions of the process of electron-beam hardening determine the approximate qualitative preservation of the chemical composition of the melted zones of alloys with respect to the alloying elements.

We must note that it is not possible to use the absolute values of theevaporation rates of the alloying elements to estimate the evaporation of the alloy. Since these elements may be present in the alloy as binary or more complex compounds, the nature of evaporation may change and its rate decrease.

Experimental studies of the process of evaporation of alloying elements with local electron-beam hardening of chrome-nickel-molybdenum steels have produced results which differ significantly from the calculated results. Thus, the rate of evaporation V_i of the substance, determined from the loss of mass of a specimen after melting, has values in the range $(0.48—14.36) \cdot 10^{-4}$ g $\cdot cm^{-2} \cdot s^{-1}$,[9] while a change in the concentration of alloying elements

was noted only for chromium. However, even this change (on the order of 0.2% by mass) in the most powerful melting conditions was too small to influence the dynamics of structural transformations. All of this indicates that for rapid heating and melting conditions, Langmuir's equation is unacceptable in view of the complexity or frequent impossibility of determining the thermophysical characteristics of the material.

Vacuum Refining and Degassing

The presence of gasses and nonmetallic inclusions in a metal, which serve as stress concentrators, always has a clearly negative influence on ductility. Processes of metal refining during electron-beam hardening involving melting of the surface in a vacuum are difficult to explain by shifting of equilibrium metallurgical reactions and increased evaporation from the surface of the melt alone.

Data are presented in[10] on degassing and refining of the metal of seams made by an electron beam in a vacuum: the quantity of oxygen was decreased by 2-3 times in comparison to the unmelted metal, of nitrogen—by 1.5-2 times, of nonmetallic inclusions—by almost two times. Their distribution in vacuum-remelted metal was quite uniform, which had a positive influence on its strength properties.

It was demonstrated in[11] that the thermal conductivity of nonmetallic inclusions at high temperatures is significantly lower than that of metals: for example, in steel it is 28 $W/(m \cdot K)^{-1}$, in SiO_2—4.7 $W/(m \cdot K)^{-1}$. In this case, the process of melting and evaporation of nonmetallic inclusions is essentially adiabatic and selective in form. The experimental data of the authors on the process of electron-beam welding of type 14KhZMA steel shows that the quantity of nonmetallic inclusions such as Al_2O_3 and SiO_2 in the seam metal is 3-4 times less than in the metal of vacuum-arc and even electric-slag remelting. The reason for this is that the time of the interaction of the electron beam with the nonmetallic inclusions in the melt is $1 \cdot 10^4$ times greater than the time of full evaporation.

We should note that electron-beam hardening with self-hardening from the liquid state usually occurs with an electron beam movement rate over the material which is significantly (an order of magnitude or more) greater than that used in welding. Thus, even if we accept a rate of movement of the electron beam on the order of 160 $m \cdot hr^{-1}$ (in[11], V = 16 $m \cdot hr^{-1}$), the time of its interaction with nonmetallic inclusions is 10^3 times greater than the time required for their complete evaporation.

Consequently, vacuum refining of metal during electron-beam hardening, accompanied by active removal of nonmetallic inclusions, is a significant factor in forming the structure of the hardened layer.

Vapor-Gas Flow Pressure

The influence of the pressure of the evaporating phase on the kinetics of the interaction of highly concentrated energy beams with metals has been noted before.[12-13] There is interest not only in a quantitative, but also a qualitative estimate of the influence of such pressures. For example, during laser treatment with an energy pulse length of $7 \cdot 10^{-9}$ s and power density of 10^9—10^{12} $W \cdot cm^{-2}$, high pressures may be created by evaporation of the metal and its cooling at extremely high cooling rates—up to 10^8 $°C \cdot s^{-1}$.[12]. We note, however, that a pressure on the order of $1 \cdot 10^3$ MPa, even at maximum flux density, yields a depth of the zone of impact hardening of not over 50 μm beneath the surface. The process of electron-beam hardening is basically different from laser treatment and treatment by relativistic electron beams. The major difference is the significantly lower energy expenditures, plus the presence of the vacuum in the treatment zone.

The maximum speed of dispersion of the vapor phase in the vacuum can be defined as[14]:

$$V_и = c_0 \cdot \exp(-L_и/RT), \quad (2)$$

or, considering the evaporated material and the energy concentration:

$$V_и = q/\rho(L_и + 2{,}5\,RT_и), \quad (3)$$

where c_0 is the speed of sound; L_i is the latent heat of evaporation. The values of V_i computed by these equations agree well with the experimental estimates of the speed of dispersion of the vapor phase away from the zone of electron-beam treatment. Thus, for iron these values are on the order of $3.1 \cdot 10^3$ $m \cdot s^{-1}$, for aluminum—$1.93 \cdot 10^3$ $m \cdot s^{-1}$.[15-16] The periodic variation in pressure over the melt resulting from the rapid dispersion of the vapor-gas phase and natural modulation of the electron beam causes a pulse pressure of up to 0.2 $GPa \cdot s^{-1}$, detected at a depth of up to 150 μm.[13]

The time of action of the "vacuum shock" is very brief—less than 10^{-3} s. However, the frequency of application of shock waves to a crystallizing solid-liquid metal volume may result in the breaking-away of peaks from the dendrites being formed and strain hardening of the thin surface layer of the solid phase. As a result, hardness on the surface of the layer may be locally increased, as had been repeatedly recorded in experimental studies.[4, 17] Consequently, based on technological considerations, modes of the electron-beam hardening process are also possible in which thin melted layers form, through which the "vacuum shock" conditions penetrate completely, thus yielding even greater hardness.

Thus, pulsed shock loading—the "vacuum shock"—is a quasi-steady process of the periodic application of shock waves to a two-phase crystallizing metal bath. The result

of this loading may be acceleration of the process of crystallization, dispersion of the structural components and the appearance in the surface layers of compressive stresses, making its contribution to the general process of electron-beam hardening.

Crystallization

With a cooling rate of the metal on the order of 10^5—10^6°C·s^{-1}, characteristic of electron-beam hardening,[17] the process of crystallization becomes essentially nonequilibrium. The formation of the structure of the hardening metal will depend largely on the rate of crystallization which grows over time and increases sharply when the solidification of the liquid metal is completed and the dimensions of the two-phase zone and, consequently, the area of the liberation of the latent heat of melting are significantly reduced. In general form, the variation in crystallization rate of the melt V_{kr} as a function of the degree of supercooling is[18]

$$V_{кр} = K\Delta T, \qquad (4)$$

where K is the kinetic coefficient of growth of the crystals. For metals, K = 0.1 m·°C^{-1}·s^{-1}; ΔT is the supercooling of the melt, °C. A numerical estimate of V_{kr} for iron, considering that

$$\Delta T = 0{,}18\, T_3, \qquad (5)$$

where T_3 is the equilibrium melt solidification temperature, °C, yields a value of V_{kr} of approximately 24-27 m·s^{-1}. These crystallization rates, considering the heterogeneous nature of the nucleation of crystals in a multicomponent alloy, determine the high degree of dispersion of structural components,[3, 14, 16] which is an additional factor in the mechanism of the hardening of alloys upon electron-beam hardening.

For iron-carbon system alloys, the supercritical cooling rates and high crystallization rates result in the formation of a small-crystal martensite structure. Since crystallization involves liberation of heat, it is possible that the newly formed martensite ages. This leads to its partial decomposition and the formation of very finely dispersed, metallographically indistinguishable carbide inclusions, additionally increasing the hardness of the crystallized phase. Hypothetically, this is an additional hardening factor in local electron-beam melting of the surfaces of alloys.

Although this hypothesis is debatable, there is indirect supporting experimental evidence. For example, x-ray structural analysis of a number of structural alloys following electron-beam hardening has shown the presence of low-carbon martensite with anomalously low tetragonality.[13] Explanation of this fact solely by the evaporation of carbon from the melting zone, without other experimental data, is unconvincing. Considering the preceding discussion and the experimentally determined high values of hardness of the martensite, its aging with conversion of the crystalline lattice to cubic form seems a more probable mechanism.

Thus, based on our analysis of the process of electron-beam hardening of alloys with melting of the surface in a vacuum, we can note the factors which significantly influence the formation of the structure of alloys.

1. Vacuum refining of the melt, accompanied by active evaporation of nonmetallic inclusions and loss of gasses.

2. Periodic pulsating loading of the crystallizing metal by the vapor-gas phase recoil pressure.

3. Rapid crystallization of the melt due to the high cooling rates, resulting in a high degree of dispersion of the structural components.

BIBLIOGRAPHY

1. E. Arata, "Heat Treatment at High Energy Density," NIHON KIKAY GAKKAY, Vol 85 No 761, 1982.

2. P. R. Strutt, "Microstructural Refinement of Hard Iron Base Materials by Laser and Electron Beam Surface Melting," METALL FORUM, Vol 4, 1982.

3. I. Artinger, M. Korakh, and N. A. Olshanskiy, "Influence of Electron-Beam Melting on Properties of Certain High-Speed Steels," TR./MEI, No 564, 1982.

4. M. V. Radchenko, N. I. Batyrev, and Ye. N. Kosonogov, "Hardening of Surface Layers of U10 steel by Electron Beam," in "Novyye metody povysheniya konstruktivnoy prochnosti stali" [New Methods of Increasing the Structural Strength of Steel], Novosibirsk, 1985.

5. G. A. Slavin, Ye. L. Mamutov, and M. V. Bulgakov, "Mathematical Model of Dendritic Crystallization of a Welding Bath," FKhOM, No 4, 1982.

6. E. Evans Kybaschewski, "Metallurgische Thermochemie," Berlin, Technik, 1959.

7. N. A. Olshanskiy, and Ye. L. Mamutov, "Vapor Pressure at the Melting Heat with Electron-Beam Welding," ELEKTRON. OBRAB. MATERIALOV, No 1, 1969.

8. M. Ardenne, "Tabellen zur angewanden physik, Bd II," Berlin, 1964.

9. M. V. Radchenko, Ye. V. Berzon, and N. I. Batyrev, "Evaporation of Metal in Electron-Beam Hardening," in "Defekty i fiziko- mekhanicheskiye svoystva splavov" [Defects and Physical-Mechanical Properties of Alloys], Barnaul, 1987.

10. T. P. Muravyeva, "Issledovaniye osobennosti struktury i svoystv svarnykh soyedineniy tolstolistovykh staley perlitnogo klassa, vypolnennykh elektronnoluchevoy svarkoy" [Study of Structure and Properties of Welded Joints in Thick-Sheet Pearlite-Class Steels made by Electron-Beam Welding], Author's Abstract of Candidate Dissertation, Moscow, 1979.

11. N. A. Olshanskiy, and M. Banasik, "Mechanism of Removal of Nonmetallic Inclusions in Electron-Beam Welding of Metals," AVTOMAT. SVARKA, No 6, 1983.

12. N. N. Rykalin, et al., "Lazernaya i elektronnoluchevaya obrabotka materialov" [Laser and Electron-Beam Treatment of Materials], Handbook, Moscow, Mashinostroyeniye, 1985.

13. M. V. Radchenko, "Structural Anomalies in Electron-Beam Treatment Melts" in "Struktura, dislokatsii i mekhanicheskiye svoystva metallov i splavov" [Structure, Dislocations and Mechanical Properties of Metals and Alloys], Sverdlovsk, 1987.

14. N. N. Rykalin, A. A. Uglov, and L. M. Anishchenko, "Vysokotemperaturnyye tekhnologicheskiye protsessy" [High-Temperature Technological Processes], Moscow, Nauka, 1986.

15. V. N. Rodigin, and V. M. Korobov, "Direct Measurement of Reactive Force Arising During Electron-Beam Welding," FKhOM, No 4, 1977.

16. A. M. Verigin, A. A. Yerokhin, V. N. Shavyrin, and V. F. Reznichenko, "Estimate of Expansion Rate of Vapor-Gas Phase Upon Deep Melting Through Metal by Electron Beam," FKhOM, No 5, 1980.

17. M. V. Radchenko, and N. I. Batyrev, "Structure Formation During Electron-Beam Hardening of 55Kh2N2MFA Steel with Surface Melting," IZV. SO AN SSSR. SER. TEKHN. NAUK., Issue 4 No 1, 1987.

18. M. K. Flemings, "Protsessy zatverdevaniya" [Hardening processes], Moscow, Mir, 1977.

UDC 658.52.001.56:621.73.043

New Automated Processes for Manufacture of Precision Hot-Forged Parts (Experience of "GAZ" Production Association)

18420192A Moscow
KUZHNECHNO-SHTAMPOVOCHNOYE PROIZVODSTVO in Russian No 3, Mar 89 pp 2-3

[Article by Ye. I. Natanzon, V. K. Malygin, V. I. Zilberberg, Yu. V. Starostin]

[Text] New waste-free and low-waste technological processes and completely automated production lines for parts and semifinished goods have been created at the Gorkiy Motor-Vehicle Plant, based on the use of: new plastic deformation processes, allowing production of highly accurate parts of various sizes and shapes, quite close in configuration to the final product; complete automation of all elements of the production of parts, including the manufacture of blanks, heating of the metal, shape modification in dies, heat treatment and, if necessary, the use of finishing operations including welding and cutting of metals; continuous production based on special new compact automated equipment installed in mechanical working shops; various priority technological and design decisions which are protected by authors' certificates.

Many years of research, experimental, planning and start-up operations have resulted in new, effective processes for the manufacture of such truck and car parts as: bed gates, wheel cylinder pistons, wheel bearing nuts, half-axles (Figure 1), differential case journal flanges (Figure 2), transmission gears, steering joint bodies and piston pins. The new processes are implemented on 20 special automatic production lines, systems and machines, manufactured and put in operation by the specialists of the Association.

The new processes are based on precise utilization of blanks, induction and (when necessary) local heating, shape change in closed-impression dies, stabilization of die tool thermal mode, and controlled cooling of forgings. These processes utilize progressive technology: the use of coiled metal, stamping of metal in the liquid state, production of forgings from welded blanks, the use of combined dies, semihot forging. The processes utilize new technical decisions: dosing of aluminum alloy, the use of a horizontal wedge die for one-pass forging of flanges on long rods in universal small presses, the use of movable dies for multiple- pass forging on universal presses, etc.

The high precision of the parts produced, complete automation of processes and organization of continuous manufacture of parts, allowing the automated equipment developed to be located in the mechanical working shops have allowed: a significant increase in material utilization and decrease in metal consumption, elimination of significant volumes of mechanical working of parts by reducing allowances and eliminating mechanical working of some surfaces; reduction in labor consumption and power consumption; significant reduction in the length of process cycles; reduction in required floor space and liberation of productive capacity for the manufacture of forgings, improving quality and usage properties of parts, eliminating heavy physical labor and radically improving the conditions of labor in the production of hot forged parts.

Introduction of the new processes and equipment has resulted in an annual savings of 6,500 tons of rolled products and an annual economic effect of 2.2 million rubles. Over 144 million parts have been manufactured since the introduction of the new equipment. Some 7,600 m^2 of forging production area has been liberated, representing a capital investment of 11.35 million rubles.

New processes and automated equipment continue to be developed. High-precision semihot forging of bevel half-axle gears has been started on two automatic production lines. An automatic high- precision forging line for diesel truck half axles is on line. A complex of automatic precision forging lines for gasoline and diesel truck pins is being installed in a unified automated production section. According to the traditional technology, the pin and flange were manufactured separately and subsequently welded together. This process is disjointed, consumes a great deal of labor, results in metal losses and large volumes of mechanical working, requiring special automatic production lines. The new process of precision manufacture of the entire crankcase pin features hot cutting of bars to produce blanks, shaping of the flange and tail portion of the pin in the hot state, heat treatment of the pin by induction heating. Introduction of the new process has liberated over 50 workers, decreasing the consumption of hot rolled products by 2,000 tons and yielding a total economic effect of at least 2 million rubles a year.

Experimental and planning-design work is continuing on precision automated forging of transmission units, steering members, shock absorber cylinders and other parts.

The processes and equipment which have been created are intended to expand the area of application of precision low-waste processes for the manufacture of a wide variety of parts by plastic deformation methods. They have important social significance, since they radically change the nature of labor in the production of forgings.

UDC 621.73.043:669.1.154

Molten-Metal Pressing of Wheel-Cylinder Pistons on Automatic Machines

18420192B Moscow
KUZHNECHNO-SHTAMPOVOCHNOYE PROIZVODSTVO in Russian No 3, Mar 89 p 5

[Article by L. S. Temyanko and Ye. I. Natanzon]

[Text] The Gorkiy Motor-Vehicle Plant previously manufactured hydraulic shoe brake pistons for trucks from D1 alloy by hot die forging with flame heating and subsequent working by cutting.

Pistons of two types with outside diameters 35 and 38.3 mm are now manufactured of type AL10V secondary metal by molten metal pressing on a special automatic machine[1]. Figure 1 shows drawings of the blanks manufactured by the traditional method a and the new method b.

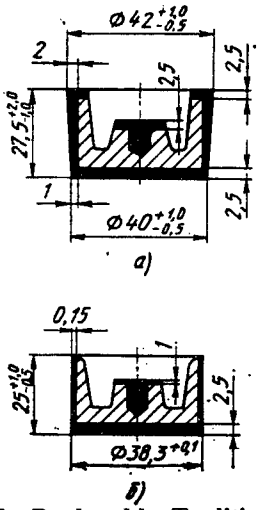

Figure 1. Blanks Produced by Traditional Method a and New Method b

The automatic machine (Figure 2) consists of pneumatically driven crank-lever press 1 for dies 2, attached to carousel stage 5, device 6 for preliminary positioning, mechanism 7 for measured dosing of portions of liquid metal from crucible 8 of the holding furnace, plus control panel 9. At the unloading position, the blanks are removed from die 2 and a lever device, actuated by pneumatic cylinder 3, pushes them onto slide 4, which transfers the blanks to their containers.

Metal Melt 1 is placed in crucible 2 (Figure 3). Portions of the melted metal are removed by a dosing unit, tube 3 and cylinder 7 with plunger 8 and spring 9. Tube 3 is immersed in the melted metal with plunger 8 in the upper position until the end of feeler 10 touches the metal surface. Compressed air is fed into cylinder 7, moving plunger 8 downward, so that the elastic liner closes the top end of tube 3. At the same time, levers 6 rotate and move the dosing unit to the position in which the metal is dumped into die 5. The compressed air is released from cylinder 7 and spring 9 raises piston 8, opening tube 3. The metal pours into die 5, the bottom portion of which is a portion of extractor 4.

After stage 5 rotates, the die containing the metal is in the operating position under press 1 (cf. Figure 2).

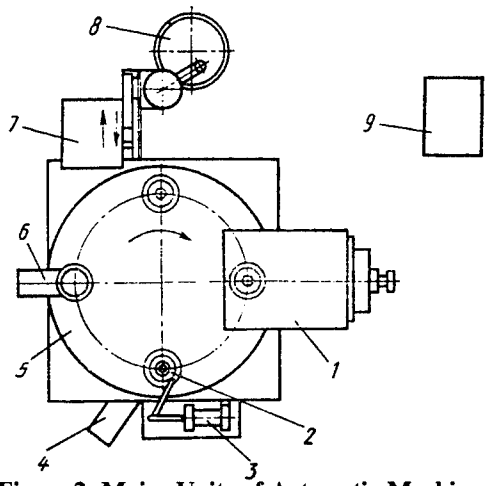

Figure 2. Major Units of Automatic Machine

When the press is switched on, compressed air enters cylinder 7 (Figure 4), piston 6 of which activates slide 3 through shaft 5 and lever mechanism 4. When slide 3 reaches its extreme lower position, the blank is shaped in die 2.

The full cycle of manufacture of a blank is completed at the unloading position, where pusher 1 raises the blank above the level of die 2. Cylinder 3 (cf. Figure 2) is engaged and the lever pushes the blank onto slide 4.

The punch, female die and pushers are lubricated with a 5% sodium chloride solution which is sprayed onto the surfaces of the tool as a fine dispersion. Before the machine is started, the die is heated to 160-180°C by

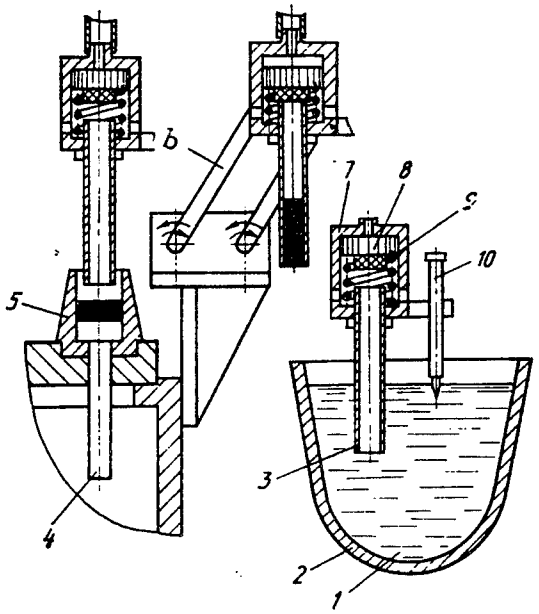

Figure 3. Diagram and Operating Principle of Molten Metal Dosing Unit

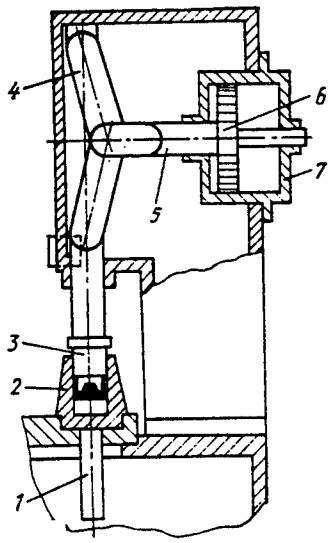

Figure 4. Diagram of Special Press

electrical coils built into the die block. The temperature of the die is automatically monitored by a thermocouple pressed into one of the dies. Dosing tube 3 (cf. Figure 3) is a calibrated section of steel water pipe with inside diameter 15 mm. Each pipe with organic silicate coating has a working life of three shifts, without coating—one shift. The dosing unit feeler is made of VK-8 metal-ceramic hard alloy. It has a working life of about one month.

Technical Characteristics of Automatic Device

Capacity of holding furnace crucible, kg	70
Press force, kN	140
Throughput, pieces per hour	330
Holding furnace power, kW	55
Dimensions, mm	3400X2650X2590

The high accuracy of blanks made by the automatic machine (0.1 mm outside diameter, cf. Figure 1) allows subsequent working to be limited to grinding. Six such automatic machines have manufactured over 61 million parts. The annual economic effect is over 105,000 rubles.

Conclusion. An automatic machine has been developed for the manufacture of wheel cylinder pistons with high accuracy. The use of molten-metal pressing decreases the metal waste and labor consumption of the manufacture of the parts. The automatic machine can be used to produce various blanks of nonferrous metals in a low-waste process.

[1] Authors' certificate number 445521, USSR, MKI V 22 d 27/12. "Carousel Installation for Molten-Metal Pressing."

UDC 658.52.011.56:621.979.001.8

Precision Forging of Truck Half Axles on Automatic Production Lines

18420192C Moscow
KUZHNECHNO-SHTAMPOVOCHNOYE PROIZVODSTVO in Russian No 3, Mar 89 pp 6-9

[Article by V. F. Lusenko, L. S. Temyanko and G. I. Stroitelev]

[Text] Truck half axles are heavily loaded parts consuming large quantities of type 40G steel. According to the traditional technology, stamping of a 158 mm diameter flange and a 48.5 mm diameter bulge at the opposite end of a forging (Figure 1.a) were performed using individual blanks 42 mm in diameter on horizontal forging machines rated at 12 and 63 MN force in several passes, involving heavy manual labor. Flame heating of 12 kg blanks before forging and normalization resulted in oxidation and decarburation of the surface layer, inefficient wastage of metal and required shot peening of forgings. Significant forging allowances were required due to forging in split dies and significant variations in dimensions of the initial blanks. The forgings (Figure 1.a) were worked on special automatic production lines. Before cutting, the forgings were straightened. The part manufacturing cycle included production of forgings and their mechanical working, requiring significant expenditures of time and manual labor.

In the new technology, half axles (Figure 1.b) for trucks are manufactured in the mechanical working shop from one-piece blanks 40 mm in diameter. The blanks are produced by cutting bars on a shear press. The manufacturing process includes the following operations, performed in sequence (Figure 2): milling (1) of the ends of the blank, preliminary centering (2) of the blank starting at the splined end with simultaneous removal of facets at both ends, induction heating (3) of the end of the blank before forging the flange, preliminary edging (4) of the heated metal and forging (5) of the flange in a single pass, water cooling of the section of the blank adjacent to the flange fillet, induction heating (6) of the end of the blank for heading of the spline end, heading (7) of the spline end (with simutaneous forming of the final center aperture), induction heating (8) of the flange rim and the spline end for normalization with subsequent cooling in air, water cooling of the flange and spline end, centering (9) of the half axle at the flange end and drilling of the aperture for production of the center at the spline end, partial working of the flange by cutting (10).

The manufacturing process is implemented on two automatic production lines[1].

Each line (Figure 3) includes: milling machine (1), machine (2) for centering and removal of facets, induction heaters (3), (6), (8) and (9), automatic machine (4) for forging of the flange with preliminary edging of the metal, sprayer installations (5) and (10), press (7) for

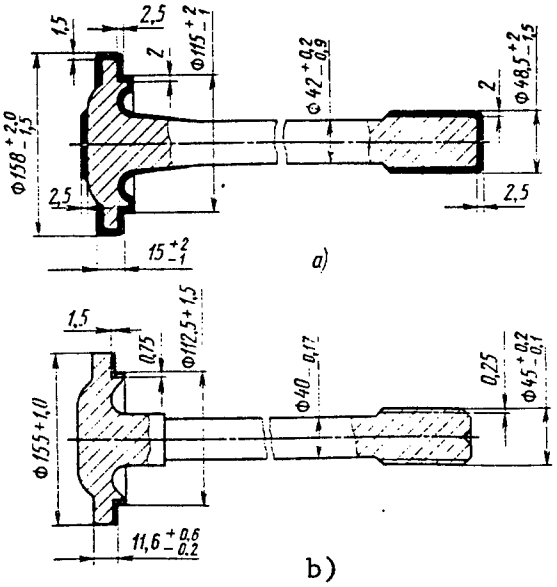

Figure 1. Truck Half Axle Forgings Made by Traditional Method

Key: (a—forging on horizontal forging machine) and new method (b—forging on automatic production line) (maching allowances indicated by bold lines)

heading the spline end, centering machine (11), plus transporter (12), hydraulic stations (13) and (14) and electrical panel (15).

The automatic machine for stamping the half-axle flange (Figure 4) consists of embossing crank press (4) model K-8342, horizontal die (2) for preliminary edging of the metal and forging of the flange, loading and unloading mechanism (1) and mechanism (3) for cooling and lubricating the die.

The horizontal die (Figure 5) for preliminary edging of the metal and stamping of the flange has cast steel box-section bed (1) attached to the stage of the embossing press. Horizontal slide (5) is mounted on the bed in guides, and carries compound die (4) in its forward portion. The rear portion of the slide has outer (n) and inner (m) chamfers at 30° to the vertical. The slide also contains a horizontal bushing and cover plate. A bracket on the bed carries vertical slide (2). It is moved by a pneumatic cylinder. This same slide carries compound die (3). The rear portion of bed (1) carries hydraulic cylinder (9), the shaft of which carries an attached tip. The stroke of the piston of cylinder (9) is adjustible. Slide (7) of the embossing press carries wedge (8), designed to interact with the external chamfer of horizontal slide (5), as well as wedge pair (6)—to interact with its inner chamfers. Wedge (8) and the bed of the die are reinforced with wear-resistant cover plates. The contacting couples of the cover plates are made of casehardened type $12KhN_3A$ steel and BrOF10-1 bonds.

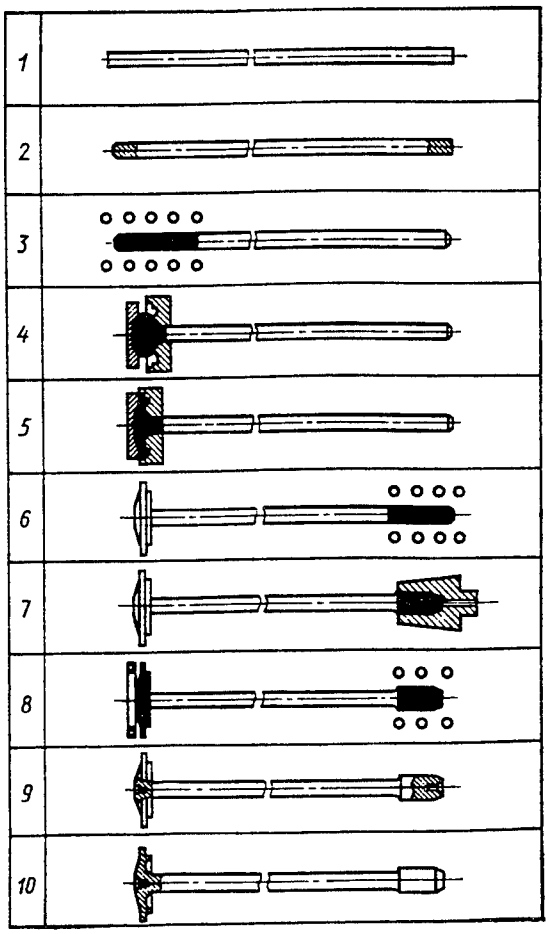

Figure 2. Technological Operations Invovled in Manufacture of Truck Half Axles on Automatic Production Line (Heated Portions of Blank and Forging Shown Dark)

The heated blank is carried by the transporter to the rollers of the loading and unloading mechanism. A pneumatic cylinder moves its carriage to the press and the blank is placed in the sleeve of the die and female die (4) of horizontal slide (5) (Figure 5.a). The carriage is removed from the press, after which the shaft of hydraulic cylinder (9) starts moving, edging the metal by means of force P (Figure 5.b) in the space between female dies (3) and (4). The shaft of cylinder (9) continues to the stop, after which slide (7) of the embossing press starts moving: the flange is forged (Figure 5.c). As slide (7) moves upward, slide (5), together with the forging, returns to its initial position. At the same time, the shaft of cylinder (9) is withdrawn and at the end of the cycle of movement of slide (5) expels the flange of the half axle from die (4) by a distance sufficient to allow slide (2) (Figure 5.d) to move upward. After slide (2) moves upward, the carriage of the loading and unloading mechanism is moved into the press, the shaft of cylinder

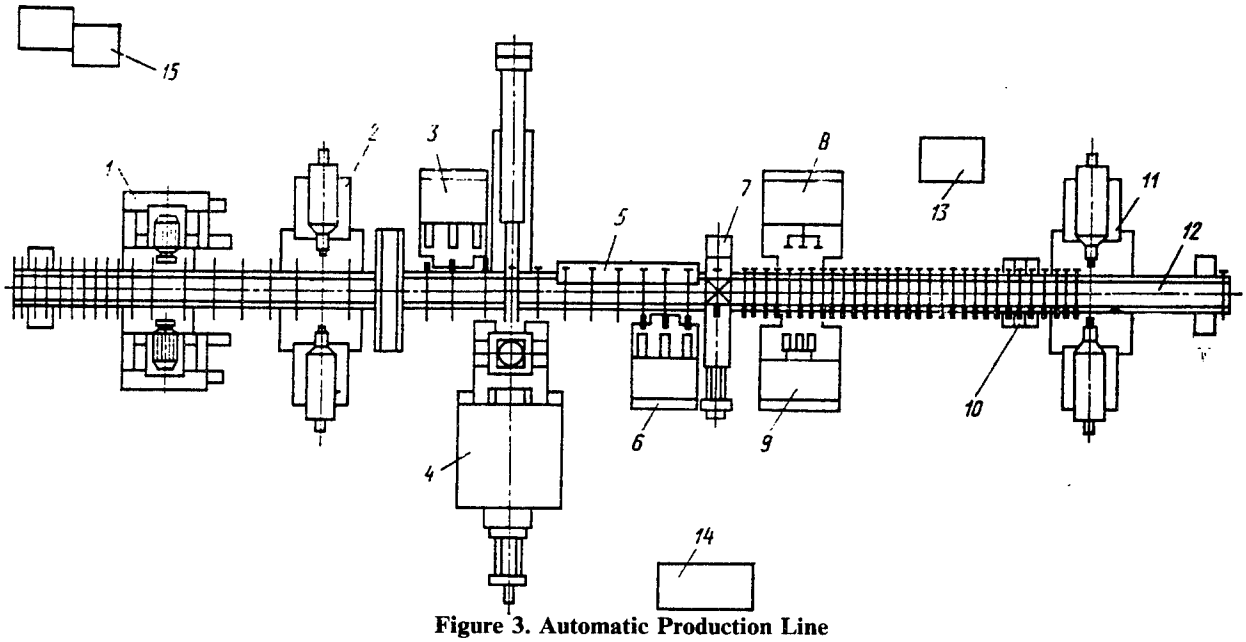

Figure 3. Automatic Production Line

(9) moves forward to its stop and expells the blank from die (4). When the flange is expelled, it acts on the chamfers of the spring-loaded clamps of the loading and unloading mechanism carriage and is clamped between them and the stop on the carriage (Figure 5.e). After this the shaft of cylinder (9) and the carriage of the loading and unloading mechanism are returned to their initial positions.

One important technological parameter of the process is deformation path S, over which the flow of the metal in the radial direction is not limited by the die cavity (Figure 5.b). The value of S determines the ability to edge the metal in this manner. If S<50- 60 mm and S>100-110 mm (for a 40 mm diameter blank) the process is virtually impossible, since in the former case great force P is required, while in the latter, the heated portion of the blank may undergo longitudinal bending.

The maximum permissible value of force P for edging the metal is limited by the need to avoid upsetting the cold portion of the blank. Force P is about 450 kN.

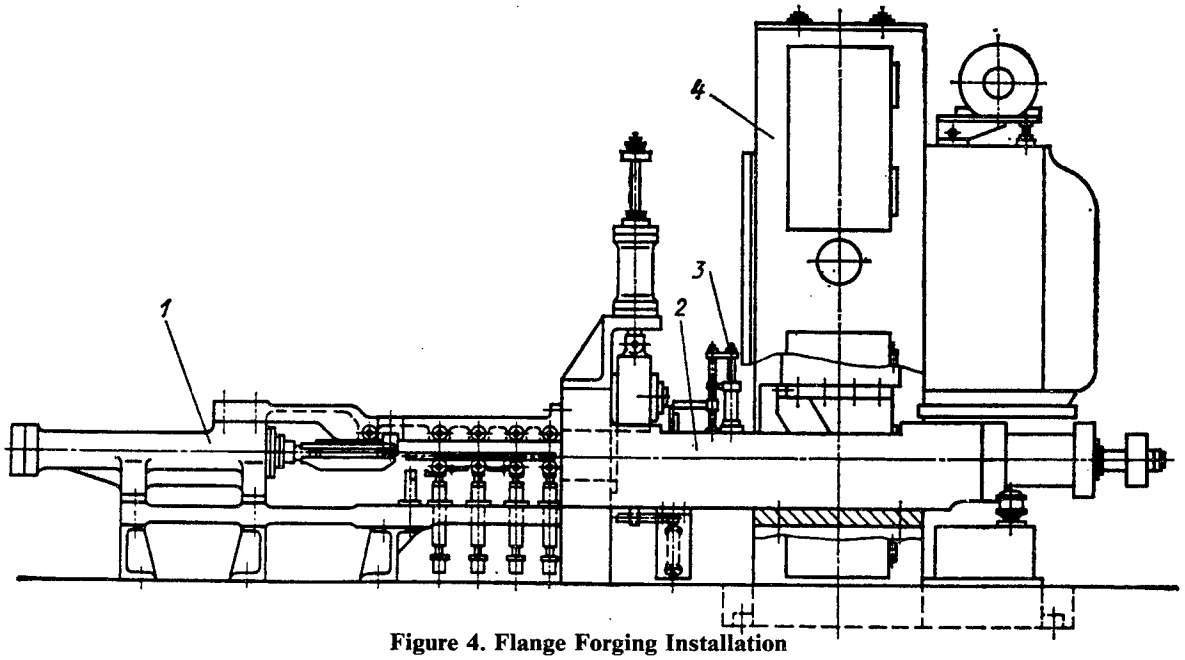

Figure 4. Flange Forging Installation

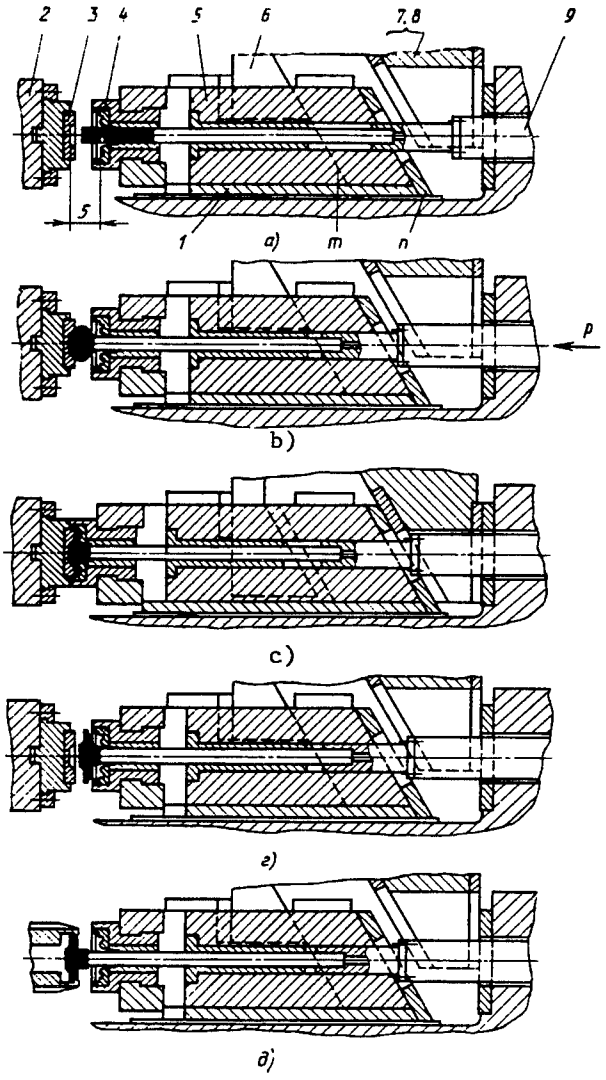

Figure 5. Characteristic Stages in Shape Change of Blank During Stamping of Half-Axle Flange (Heated Portion Shown Black)

Under normal conditions (optimal blank temperature, proper lubrication and cooling of dies), the force of deformation required to edge the metal is 100-200 kN.

The speed of movement of the shaft of cylinder (9) during edging the metal is not over 70 mm/s. Deformation force P during forging of the flange is up to 7 MN.

The press used to head the spline end of the forging (Figure 6) is melted on a common slab and has longitudinal uprights connected by bars. The slab carries the base with prisms (1) for placement and fixation of the semifinished blank with its forged flange. The press upright carries hydraulic cylinder (7), the shaft of which is connected to traverse (6). The travel of the shaft of cylinder (7) and traverse (6) is adjustible. The traverse carries compound die (5). Traverse (6) is connected to spindle (4), which carries cams closing the vertical movement of traverse (2) and prism (3) which is connected to it.

The blank, heated at one end, is placed on prism (1) by the transport device. As the shaft of cylinder (7) moves, first vertical traverse (2) and prisms (3) descend. As traverse (6) continues to move, the bulge is formed in the die. Traverse (6) moves at 70 mm/s. The force involved is 200-300 kN.

All machines (cf. Figure 3) used to cut the blank are two-way machines with two-speed mechanically driven stages. The machines are equipped with pneumatic clamps.

The induction heaters are made on carriages which move across the longtudinal axis of the production line. The inductors consist of three series-connected sections: a solenoid section with heat- resistant liner to heat the blanks before forging the flange and before heading, and also to normalize the spline bulge and single- turn heaters with magnetic circuit to normalize the flange.

The design of the transporter allows movement of blanks, semifinished pieces and forgings in steps in the first and second parts of the production line in separate phases, allowing the power supplies of the heaters in the first half of the line to be used for the heaters in the second half as well.

The die inserts which form the flange and bulge are made of ZI958 steel, hardened (43.5-47 HRC_e) and nitrided to a depth of 0.3-0.5 mm in the engraved portion. Shape formation of the central aperture at the spline bulge end is performed by a hard metal-ceramic VK8 alloy punch. The mean life of inserts used to form the inner surface of the flange is 2500 forgings, of those used to form the outer surface—4,000 forgings. The die used to forge the spline bulge has a life of about 50,000 forgings. They are cooled by running water. The inserts which form the outer surface of the flange are resurfaced twice. After the first and second operations their life is 2500 and 1500 forgings, respectively. The production line uses water cooling of forging tools which form the shape of the flange by spraying. The inner surface of die (3) (Figure 5.a) which edges the metal is lubricated by type OGV-75 water-graphite material. The concentrate is diluted with water 1:10 (by volume). The mixture is applied by compressed air and sprayers.

Technical Characteristics of Line

Press force, KN:	
flange forging	16,000
hydraulic	850
Power to heat blanks, kW:	
for stamping and normalizing flange	250
for heading and normalizing spline end	100
Throughput, pieces/hr	150
Dimensions of line, mm	23,500X9800X4135

The table presents the basic technical and economic characteristics achieved by the use of the traditional and new technologies.

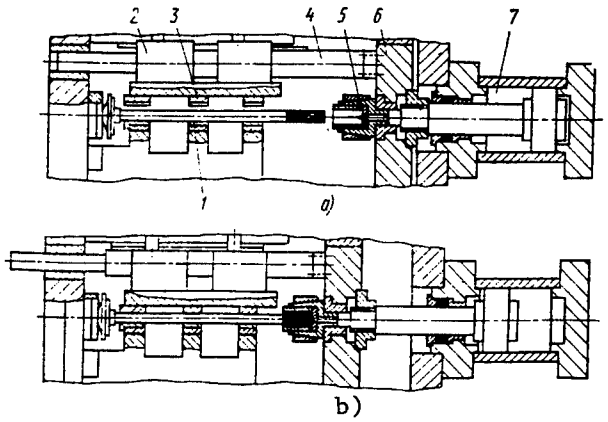

Figure 6. Diagram of operation of die for manfacture of spline end of half axle:

Key: a—initial position; b—final stage (heated portion of blank shown in black)

The manufacture of half axles by the new technology has allowed the mass of the finished product to be reduced, while assuring precise forging of the flange and heading of the spline bulge of the half axle. The consumption of metal per part has been decreased by 1.95 kg by decreasing the machining allowance and eliminating working of the surfaces of the chamfers, outer plane of the flange, end and facets of the spline bulge (Figure 1). The allowance for machining the spline thickening was about 0.25 mm per side, which permits it to be worked by grinding alone. The high accuracy and smoothness of the surface of the centering aprature, forged simultaneously with the spline bulge, allows it to be used to center the half axle for all subsequent cutting operations.

Technical-Economic Characteristics

Technology Characteristic	Traditional	New Automatic
Mass, kg:		
half axle	12.0	10.8
blank	13.3	11.3
chips produced by cutting one forging	1.2	0.5
Metal consumed for 1000 parts, kg	13,659	11,634
Labor consumption, %	100	35
Consumption of gas per 1000 parts, m^3	56,515	—
Consumption of electric power per 1000 parts, kW·, hr	1506.3	2720
Cost of all energy consumption per 1000 parts, r	87.59	13.53
Consumption of metal for forging tools per 1000 parts, kg	70.8	7.4
Production area, m^2	1350	720
Technological Cycle Length, hr	9	0.6
Number of parts simulaneously in production	2100	69

The new method of manufacturing half axles has decreased transportation costs, reduced labor consumption by a factor of 3, the length of the manufacturing cycle by a factor of 15, production area required by a factor of 2. The manufacture of half axles no longer involves the forging shop, releasing the facility for the production of 10,000 tons of forgings per year. One automatic mechanical working line and five automatic lines used to expand production are no longer required. Equipment costs have been divided by 3. The new process eliminates the use of gas fuel and decreases energy costs by a factor of 6.5. The cost of forging and cutting tools has been decreased. More than 7 million half axles have been manufactured on two automatic production lines.

The annual economic effect is 698,000 rubles. The consumption of rolled products is reduced by 1200 tons per year.

[1] Authors certificate 547276, USSR, MKI B 21 J 5/08; B 21 D 43/06. "Automatic Production Line for Manufacture of Half Axles."

UDC 658.52.001.56:621.974.813.001 8

Semihot Stamping of Gears on Automatic Production Lines

18420192D Moscow
KUZHNECHNO-SHTAMPOVOCHNOYE PROIZVODSTVO in Russian No 3, Mar 89 pp 13-14

[Article by Ye. I. Natanzon, L. S. Temyanko, Yu. I. Gyubin]

[Text] The gear wheels for second gear of the GAZ-53 truck transmission (Figure 1.a) were manufactured by die forging on a horizontal forging machine with metal utilization factor 0.494. Preliminary lathe working of the forgings required eight semiautomatic machines occupying a production area of 200 m^2.

The new technology[1] manufactures blanks (Figure 1.b) with smaller machining allowance.

The initial blanks of type 35 Kh steel are produced by cutting hot-rolled bars 56 mm in diameter on shear presses. The ends are cut to assure high accuracy of dimensions and volumes of the blanks. The losses of metal and labor consumption are compensated by the ability to produce very accurate forgings. Semihot forging of blanks at 860°C is performed in three passes in a special closed impression. By accurately centering the

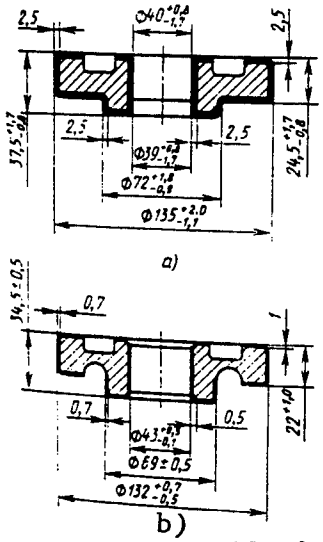

Figure 1. Gear Wheel Forgings Manufactured by Hot Die Forging (a) and Semihot Forging (b)

blank (Figure 2.a), it is possible to produce an axisymmetrical intermediate product (Figure 2.b) with a nonpenetrating cavity for broaching (Figure 2.c). During the finishing pass of forging, first the nonpenetrating cavity is made, then the forging is shaped (Figure 2.d) with the penetrating hole.

Figure 3 shows the design of the die for multiple-pass forging. Press stage (1) carries slab (2). Slab (2) carries die slab (3) in guides. A hydraulic cylinder is provided to move the die in the horizontal direction along slab (2). Slabs (8) and (9) are connected by columns and sleeves with slab (3). These slabs have two positions fixed relative to slab (2).

With the die in the extreme right position (Figure 3), the press slide acts only on top slab (8), causing slab (7) to move down along with punches (6) and (14), used in the first and second forging passes. Die forging of the initial blank occurs in female die (5); shaping of the nonpenetrating cavity for broaching of the aperture occurs in female die (18). During the return stroke of the slide, the semifinished products are removed from dies (6) and (18) by ejector (4), (21) and (19), (20) by the action of the press pusher. Upper slab (19) and the die elements connected with it remain stationary.

By the time the slide reaches its uppermost position, the initial blank and semifinished products from the first and second passes have been grasped by gripper (13), and the die moves along slab (2) to the extreme left position. The gripper moves to the left and its clamps spread, the initial blank is placed in die (5), the semifinished product from the first pass is placed in area (17), while the semifinished product of the second pass is placed in die (18). The axes of symmetry of broach (10), extractor (11), die (12), punch (15) and extractor (16) of the third forging pass now match the axis of the press. Slab (9) is coupled to the upper forging slab and the next

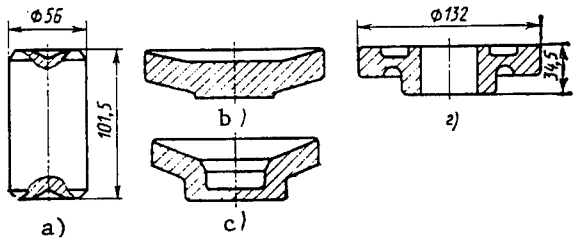

Figure 2. Forging Transitions

press stroke starts. Broach (10) cuts out a blank which is driven by compressed air through channels in slab (3) into a container, while punch (15) shapes the forging in die (12). During the reverse stroke of the press slide, the forging is removed by extractors (11) and (16) from die (12) and placed in the position to be clamped by gripper (13). It is removed from the working area. Slab (9) is released, the die shifts to the right with the initial blank in female die (5). The semifinished product of the first pass is retained over area (17) and, when the clamps of the gripper spread it drops into die (18). The cycle is then repeated.

The sequence of operations and movements of the gripper device and die set are shown in Figure 4.

Rotator (2) places initial blank (3) above the female die for the first pass. Die (1), clamps (4) and (5) of the gripper are in the far left position (Figure 4.a).

Clamps (4) and (5) are shifted to the right by 330 mm (Figure 4.b), the die set shifts to the left by 550 mm (Figure 4.c), i.e., the first and second forging passes occur.

Clamps (4) and (5) shift to the left (Figure 4.d) by 220 mm and hold the semifinished product from the first and second pass.

Clamps (4) and (5) move the semifinished product to the left (Figure 4.e) by 110 mm. The die shifts left (Figure 4.f) by 550 mm, i.e., the third forging pass occurs.

The automatic line for semihot forging of gear wheels (Figure 5) consists of automatic loader (1), two-way, four-spindle automatic machine (2) for simultaneous two-way cutting of blanks and removing of facets, induction heater (3) based on a model TPCh-250-2.4 thyristor converter, manipulator (4) to feed the heated blanks into the die set, installation (5) for multiple-pass forging on the embossing press, conveyer (6), machine (7) for two-way removal of facets in the forged aperture, hydraulic stations (8) and (11), high-frequency power supply (9) and electric control panels (10).

Loader (1) consists of electromagnets to feed the initial blanks from the container and a vibration feeder to orient each blank to automatic machine (2). The blanks in induction heater (3) are moved by a pneumatic pusher. Induction heater (3) is equipped with a device to reject insufficiently heated blanks. The manipulator

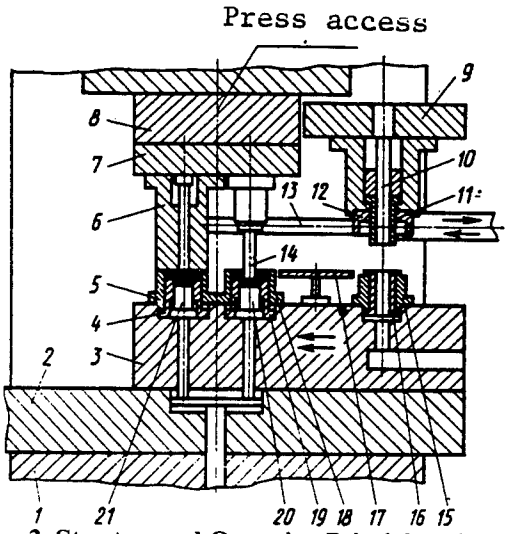

Figure 3. Structure and Operating Principles of Multiple-Pass Die Set

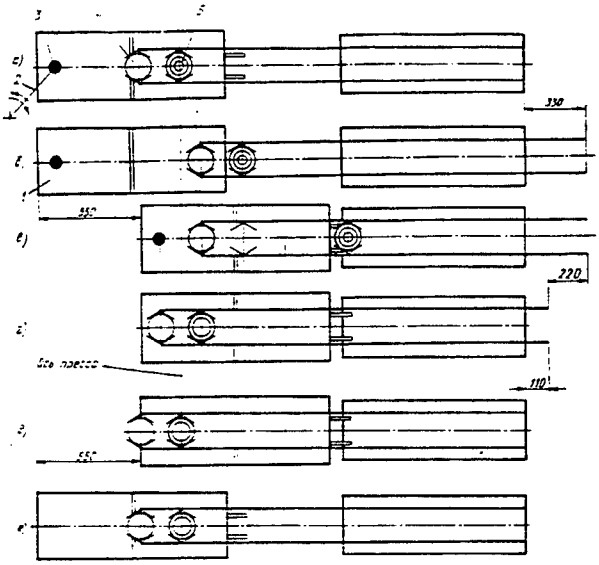

Figure 4. Characteristic Positions of Die Set and Gripper Clamps

which feeds the heated blanks into the die set is mechanically connected to a sprayer device to cool the die tool after the first and second passes: when the hot blank is placed in the die set, the sprayer is extracted from the die. Forgings on conveyer (6) are cooled by air to 500-600°C, then by water to 60-80°C. Machines (7) for removal of facets in the apertures of the parts are based on universal drilling machines.

Technical Characteristics of Line

Press force, MN	16
Heater power, kW	250
Current frequency, kHz	2.4
Throughput, pieces per hour	300
Dimensions, mm	22,000X6045X4780

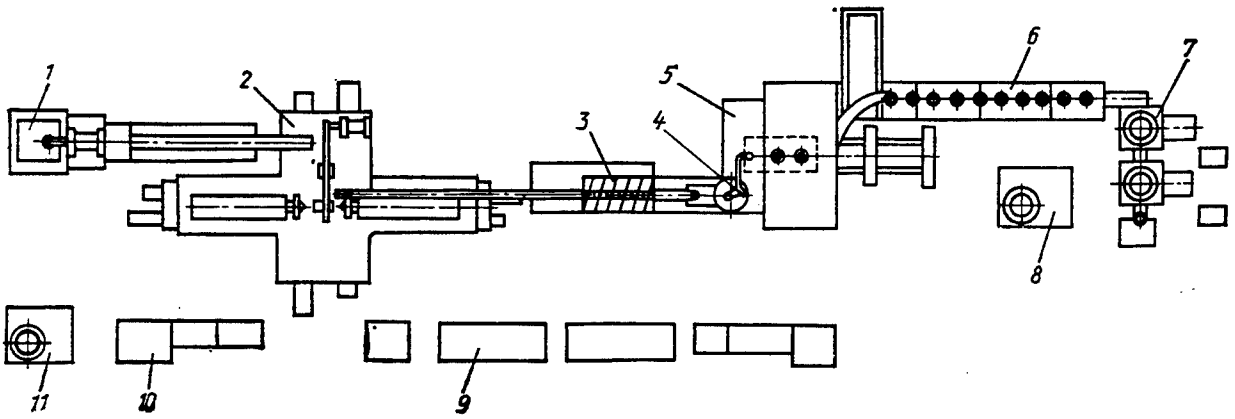

Figure 5. Arrangement of Technological Equipment and Elements of Combined Automatic Production Line

Table 1

Loss elements	Horizontal forging machine	Automatic line
Adjustment and process wastes	0.038	0.048
End wastes	0.368	—
Chips from preliminary cutting	0.510	—
Cutting ends of incoming blanks	—	0.135
Mark for broaching aperture	—	0.068
Machining allowance	0.242	—
Total losses	1.158	0.251

Table 2

Characteristic	Horizontal forging machine	Automatic line
Metal utilization factor	0.49	0.71
Metal consumption, t	2351	1654
Gas consumption m^3:		
heating for forging	991,000	—
for normalizing	254,000	—
Electric power consumption, kW·hr:		
heating for forging	—	630,000
for turning	362,040	—
Labor consumption of modified technological process, standard hours	30,492	6,985

The forgings produced on the line have high accuracy and small machining allowances (0.7 mm for outer surfaces and 0.5 mm for central aperture), 1.5-2 times less than the allowances for similar forgings produced on domestic and foreign automatic hot-forging equipment.

This has allowed the metal utilization factor to be increased to 0.71 and has eliminated preliminary mechanical working on the eight lathes.

The metal losses (kg) involved in manufacturing the gear wheel are shown in Table 1.

Table 2 shows the technical and economic characteristics of manufacture of the blanks (in a program of 782,000 blanks).

The automatic line for production of gear wheel blanks has been installed in a mechanical working shop. In addition to releasing sufficient area for the manufacture of 2000 tons of forgings per year in the forging shop, the required area in the mechanical working shop did not increase. Since its installation, more than 1.5 million parts have been manufactured. The annual savings has been 160,000 rubles, plus 700 tons of rolled metal.

An automated combined line has been created and is in successful use for the manufacture of blanks for gear wheels to be used in a truck transmission.

[1] Authors' certificate No. 1147509, USSR MKI B 21 J 13/02. "Installation for Multiple-Pass Forging."

UDC 621.735.001.8

Low-Waste Processes for Manufacture of Gear Wheel Blanks

18420192E Moscow
KUZHNECHNO-SHTAMPOVOCHNOYE PROIZVODSTVO in Russian No 3, Mar 89 pp 16-17

[Article by A. S. Kalashnikov, Yu. N. Sergeev, L. G. Sharoyan-Saringulyan]

[Text] Efficient utilization of material is traditionally one of the basic thrusts of the technological policy of the Moscow Motor Vehicle Plant imeni I. A. Likhachev. The consumption of metal is significantly reduced by the transition to low-waste technological processes for manufacture of blanks, the dimensions of which are as close as possible to the dimensions of the finished product. The area of use of low-waste technological processes is continually expanding, extending to parts of complex shape such as transmission parts.

Hot forging is used to produce bevel gear blanks with both straight-cut and helical teeth (Figure 1). Low-waste technological processes for the manufacture of bevel

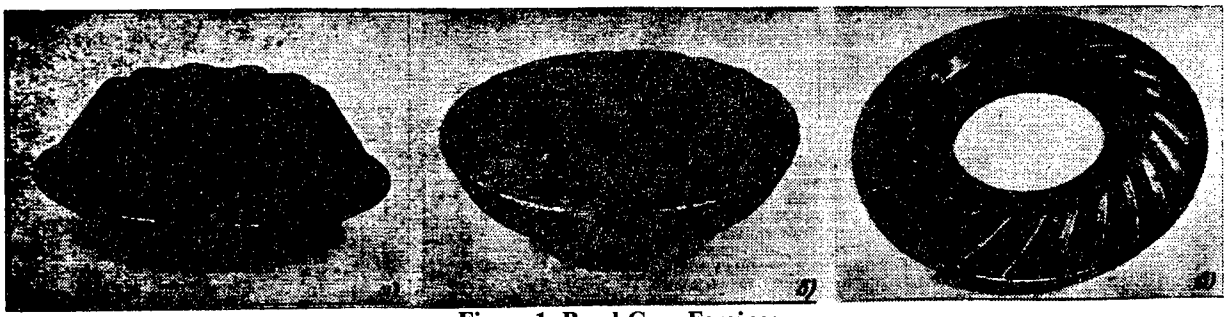

Figure 1. Bevel Gear Forgings:

Key: a—differential satellite gear; b—half-axle gear; c—bevel drive gear

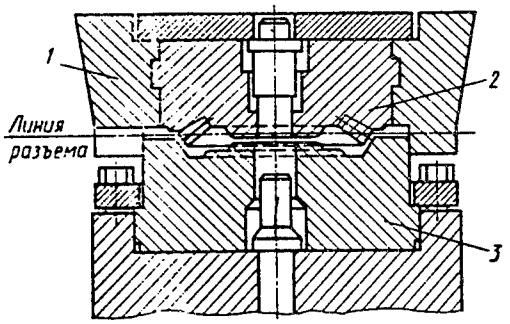

Figure 2. Operating Die Inserts for Hot Forging Crank Press

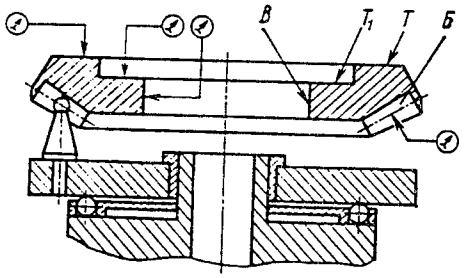

Figure 3. Diagram of Checking of Bevel Gear Forgings

gears have been developed by the ZIL plant in cooperation with the Scientific Research Institute for the Motor-Vehicle Industry. The gear profile includes a machining allowance, required for finishing of the gear teeth.

Bevel gear blanks are forged on hot forging crank presses with nominal force ratings of 16, 25, 40 and 63 MN. The blanks for forging are cut from 50-100 mm diameter bars on shear presses with mass variation plus or minus 30 g. The blanks, preliminarily heated in induction furnaces to 1230-1260°C, are forged in two passes (upsetting and final forging with tooth shaping). Upsetting is necessary to remove scale and adjust the diameter of the blank to the approximate diameter of the forging.

The inserts used in hot forging crank presses are planned so that the maximum diameter of the bevel gear forging is located in the plane of the separation (Figure 2). A "locked" insert design, in which the top (toothed) insert (2) with ring clamp (1) is centered with respect to the outside diameter of lower insert (3), is required for production of good quality forgings. The gap betwen the upper and lower inserts is 0.2-0.3 mm. This design eliminates the possibility of significant shifting of the halves of the die in the separation plane.

The main part of the die is the toothed insert, which forms the shape of the gear teeth. The gear inserts are produced by precision casting using the technology developed at the Motor Vehicle Scientific Research Institute.

The life of the cast toothed inserts for forging of satellite differential gears and half-axle gears is 3.5-6.0 thousand forgings, for stamping of driving bevel gears—1.5-2 thousand forgings. As low-waste processes are introduced and statistical data on the life of toothed inserts is accumulated, it is best to change dies on a schedule, eliminating the production of defective forgings unsuitable for subsequent mechanical working.

After forging, systematic checking of the quality of forgings with preforged teeth is required. Visual inspection is used to check for the presence of defects, then the height of the forging, its outside diameter, flash size and aperture diameter are measured.

The gear wheels are checked using special indicator-type measurement devices. Gear forgings are placed (Figure 3) on three to five spherical pin supports and the variation of the allowance is tested by checking the tooth profile, variation in positions (T) and (T^1) of the teeth and aperture (B).

The most important operation in the low-waste technological process is the first one. In this operation, the intermediate bases are generated—the aperture, ends of the gear face and hub, outside diameter of hub, etc. The accuracy of relative placement of these surfaces and their placement with respect to the lateral surfaces of the teeth are determined in this stage. The layer of metal removeod from the supporting end of the gear wheel in the first operations must be particularly carefully checked, since it determines the tolerance at the base of each trough and the lateral surfaces of the teeth.

The working of the teeth on forgings is difficult due to variations in the allowance over the side surfaces and at the bottom of the troughs of the teeth, the presence of scale and the decarburized layer (Figure 4).

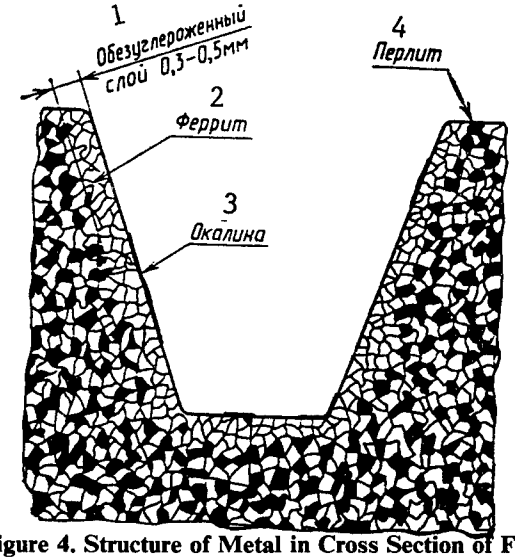

Figure 4. Structure of Metal in Cross Section of Forged Tooth:

Key: 1—decarburized layer; 2—ferrite; 3—scale; 4—pearlite

Under mass production conditions it is difficult to assure a constant machining allowance on teeth obtained by hot forging. Increasing the tolerance on the profile and at the bottom of the trough of the teeth as each die wears increases the load on the primary broaching cutters and intensifies their wear. The use of a starting portion on the first blades of broaches can avoid shock in the kinematic chain of a machine and increase tool life.

Scale on the surface of forged teeth causes damage to and cracking of the cutting edges of milling tools. Careful scale removal is required, usually performed in shot-peening chambers by shot 0.8-1.1 mm in diameter.

The decarburized layer also causes significant deterioration of cutting conditions. The ferrite structure of the decarburized layer is quite tough, causing adhesion of chips to the cutting edges of tools: the roughness of the lateral tooth surfaces is increased, the life of the cutting tools is decreased.

As teeth are formed in the forging process, a secondary fiber structure is developed, oriented along the tooth profile. As gears are used, this directed fiber structure increases the strength and wear resistance of the teeth. Whereas in straight-cut bevel gears used in truck differentials, operating under static loads the strength characteristics increase by only 5-10%, in helical-cut bevel gears, which experience primarily bending loads, strength is increased by 20-25%.

Introduction of low-waste technological processes for the manufacture of bevel gears at the ZIL plant and its affiliates has reduced the consumption of alloy steel per part by 0.37-1.3 kg. The annual savings of rolled products has been 1,644 tons, the total annual economic effect over 793,000 rubles.

UDC 621.983.073:658.524

Problems of Short-Run Sheet Cold-Forging Production and Their Solution

18420192F Moscow
KUZHNECHNO-SHTAMPOVOCHNOYE PROIZVODSTVO in Russian No 3, Mar 89 pp 32-34

[Article by I. A. Chikin, K. Yu. Khalturin]

[Text] The list of parts manufactured by cold sheet forging in the chassis forging shop includes over 7,000 items. The manufacturing process involves short production runs; parts manufactured in series of medium length represent not over 3% of the total production.

There are difficulties in the operation of this shop: when manufacturing forged parts for new products, a great number of special and expensive dies are required; the time required to manufacture products is increased; it is difficult to automate the second, third and fourth forging operations, which consume the most labor and represent the greatest danger of injury.

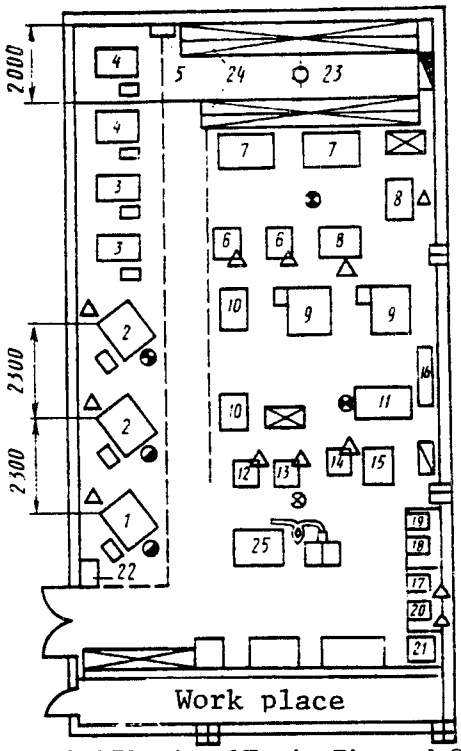

Technological Planning of Forging Piecework Section:
Key: 1, 2, 3 and 4—Crank presses rated at 630, 400, 250 and 160 kN; 5—Equipment card file cabinet; 6—25 kN crank press; 7—Model 959.29.000 multiple-position press; 8—Guillotine cutter model MA-402.00.000; 9 and 10—Model 25e-1383ChPO and Ug D2009 bending machines; 11—Model RUYe-63 hydraulic press; 12, 13 and 14—Cutters: corner, radial and slot models 1077.382.830.002, 1077.382.250.001 and 1077.383.850.002; 15—Bench plate; 16—Model Ug. 04.094 technicians bench; 17—Pneumatic tabletop press model OA-1053; 18—Tabletop drilling machine; 19—Thread-cutting machine; 20—Tabletop lever press; 21—Model ZB632 grinder; 22—Waste container; 23—Model KShO- 0.125 stacking cranne; 24—Die shelves; 25—Model GDU-16 installation

In order to solve these problems, a combined creative mixed team was set up, and a policy on mixed combined creative teams involved in the development, assimilation and utilization of flexible production systems was developed. The team included qualified workers: adjusters, technicians, forging machine operators, milling machine operators, lathe operators, contollers and engineering- technical workers: technologists, designers, electronic engineers; the team is headed by the forging flexible production system chief designer.

The flexible production system combined creative mixed team had two tasks: organize two sections—a piecework forging section and a robot-controlled forging section, in order to create the elements for a control flexible production system for the chassis-forging facility.

After four years of work, the control combined creative mixed team created a piecework forging section. Each part in piecework forging is produced in several operations, and any complex contour or profile is formed in sequence by combining individual simple elements. Each of these simple elements is forged by a universal die designed for the production of elements of just that contour or profile of various sizes.

Various combinations of simple elements can be used to produce a great variety of very complex parts. Thus, with a limited number of dies it is possible to produce parts of great complexity.

The piecework forging section, with an area of 136 m^2, is located outside the main production area of the chassis-forging shop. This section contains 22 units of process equipment, 14 of which are specialized process equipment planned and manufactured by the combined creative mixed team. The section includes a mechanized stacking storage area for storage of universal equipment: dies, blocks, cassettes and interchangeable tool sets (1,580 items in all). For comparison: the piecework forging section at LOMO plant, which has been in existence for over 30 years, has 7,000 units of equipment, while the piecework forging section of "Volna" production association (in Novgorod), which has been in existence over 15 years, has 5,000 units of equipment.

Design-technological, standard-methodological and organizational documents have been developed for the piecework forging section, defining the system used to prepare for production of stamped parts of new products with the minimum cost of manufacture of stamping equipment and the maximum reduction in the time required to master and prepare for production.

Particular attention should be given to the "classifier of technological capabilities of universal equipment in the piecework forging section," Ug0.091.036, intended for use by designers, the chief technologist's service and shop technolgists. It presents the technological capabilities of each unit of universal equipment. Parts for piecework forging are selected considering the recommendations of the nomogram, i.e., the economic expediency of various methods of manufacturing parts. The classifier consists of eight sections:

I—Universal dies and equipment for cutting of blanks.

II—Universal stamps and equipment for cutting of contour elements.

III—Universal dies and equipment for piercing.

IV—Universal dies and equipment for bending.

V—Universal dies for various operations: straightening, flanging, etc.;

VI—Adjustment for model KO-126AP numerically programmed press.

VII—Adjustment for model PKR-1 press.

VIII—Set of tools for model RKKhA-40 and Le-100-1-3000/n edge- bending presses

The accompanying figures shows the technological planning of the piecework forging section.

The piecework forging section has produced 2,816 forged parts for new products, thus eliminating the need to create 2,800 special dies.

Hydrodynamic forging using model GDU-16 installations has not been successfully introduced due to the low quality of the installation itself and the unavailability of specific recommendations by the manufacturer for planning of equipment.

Forging of parts has been introduced using model KO-126AP and KO-126P numerically controlled piercing presses. These presses are used to manufacture parts with frequently repeated identical elements, basically parts such as "panel," "barrier," and "wall."

During the first stage of creation of flexible production system elements, the chassis-forging shop created and put in use a flexible production system for cold sheet stamping of tool parts.

The need to create the flexible production system was determined by the rapid rate of scientific and technical progess which in turn requires dynamic renewal of the design of tools with a continuous decrease in the share of series production. Therefore, traditional methods and equipment for rigid automation lose their advantages and are replaced by industrial robots and manipulators, robot systems and numerically controlled equipment, automated transportation and storage, supplementary and other systems.

The flexible production system includes: a robot-operated model RSK-250 storage system, in which forging equipment is stored and retrieved as needed. Dies are manufactured or modified according to requirements for their design as needed for robot-operated forging; the GPM-1 flexible production module, consisting of a model KD2124E 250 kN press, a model MP-9S industrial robot, and a translational- rotational feeder-pusher. The GPM-1 can perform 179 operations. As its operation has demonstrated, the design of the module is reliable, and a duplicate is planned for the future; a flexible production module type GPM-2, consisting of a model KD2124E 250 kN press, and a model MP-9S industrial robot; a vibration-hopper feeder. The GPM-2 can perform 23 operations. Loading of parts does not require preliminary orientation or packaging of blanks. The use of the built-in vibration trough as an intermediate link between the vibration hopper and the starting position for clamping of parts by the industrial robot has stabilized the operation of the module, increasing the reliability of feeding of blanks to be retrieved by the industrial robot; the flexible production module GPM-3, consisting of a model KD2124 250 kN

press, model MP-9S industrial robot and translational-rotational pusher feeder. The GPM-3 can perform 96 operations. One peculiarity of this module is that it includes a universal block with interchangeable packets allowing 33 operations to be performed; a flexible production module type GPM-4, consisting of a model KD2330 1,000 kN press, model BRIG-10 industrial robot and bottom feeder. The GPM-4 can perform three operations; a flexible production module type GPM-5, consisting of a model KD2328 630 kN press, model BRIG-10 industrial robot and bottom feeder. The GPM-4 can perform 24 operations; a flexible production module type GPM-6, consisting of two model KD2124 250 kN presses. It was planned for use with a three-armed robot (a modernized model MP-9S). The results of testing were negative—the module was not introduced. The GPM-6 is now being redesigned; a flexible production module type GPM-7 for rolling down burrs on transformer-iron plates, consisting of rollers and a modernized two-arm model MP-9S industrial robot. The GPM-7 has mastered 10 operations; a flexible production module type GPM-8 for cutting of "screen" type parts. It consists of an edge-cutting machine designed by the unit, equipped with model MP-9S industrial robots, plus a vibration-hopper feeder. The GPM-8 has mastered two operations; a flexible production module type GPM-9 consisting of a model KD2322 160 kN press, a model MP-9S industrial robot, vibration- hopper and shaft feeders. This module has been introduced to production, and is now in the adjustment stage, and has mastered one operation; a flexible production line consisting of two model KD2124E 250 kN presses, five model MP-9S industrial robots and two feeders—a translational-rotational pusher and vibration-hopper device located to the left and the right of the presses. Forging can be performed either from left to right or from right to left. The flexible production line has mastered 22 operations; a transportation system based on a "GNOM" small electric loader with lifting capacity 250 kg, powered by an electric power line; a control system, including a system to control the robot-operated storage area, supporting automatic loading and unloading of technological equipment at a specified address, cycling of robots and sensors, monitoring the positions of clamps, removal of parts, and a set of grips of various designs.

The most labor-consuming and dangerous operations in forging are now performed by robots: bending, shaping, piercing, straightening, embossing and cutting.

The flexible production system is serviced by two forging machine operators and one adjuster.

The modules described above are used for the production of additional types of parts each month. Mastery of new operations and adjustment of the equipment are performed by combined creative mixed team member workers under the supervision of designers and technologists.

The GPK created is a necessary stage in the creation of a forging flexible production system.

The four years of activity of the combined creative mixed team have decreased labor consumption by 404,114.2 standard hours; the economic effect has been 944,556 rubles; 20 standard production worker positions have been eliminated.

UDC 62.86:621.38

EMAGO-097 Device for Orientation of Flat Ferromagnetic Blanks

18420192G Moscow
KUZHNECHNO-SHTAMPOVOCHNOYE
PROIZVODSTVO in Russian No 3, Mar 89 pp 34-35

[Article by A. V. Polis]

[Text] Automation of forging operations in machine building and electrical product manufacture is frequently hindered by the unavailability of devices to orient blanks to be seized by a manipulator. This equipment must be universal for use in series and short-run production situations.

Universal devices can be created to orient ferromagnetic blanks, utilizing the force of an electromagnetic field. The highly universal nature of electromagnetic orienting devices results from the contactless action on the parts. The shape and size of the orienting organ and orienting part therefore need not be rigidly matched.

Orientation of most flat blanks involves their reorientation by 180° (flipping). To do this, a fixing force is applied to the end of a part, with a flipping moment applied to the remainder of the part. Blanks can be manipulated by a properly distributed magnetic field. Field sources include special electromagnetic systems—electromagnetic flippers (reorienters).

Such magnetic systems have been developed at the Institute of Physics, Latvian Academy of Sciences. Electromagnetic reorienters are used in the EMAGO-097 device, designed for orientation of flat ferromagnetic blanks.

The dimensions of the parts oriented are as follows: minimum 0.1X3X6 mm, maximum—10X60X120 mm.

The EMAGO-097 orientation device consists of a sloping trough equipped with devices to recognize the position of a part and universal actuating mechanism—an electromagnetic flipper. The device utilizes various means for recognition. Devices can be recognized by means of a set of interchangeable standard patterns (Figure 1). In this case, the electromagnetic flipper is switched on as each part is fed through. Depending on the initial position of the part, it is either reoriented or the pattern prevents reorientation. After this, the electromagnetic system is switched off and the part continues to slide down the trough under its own weight.

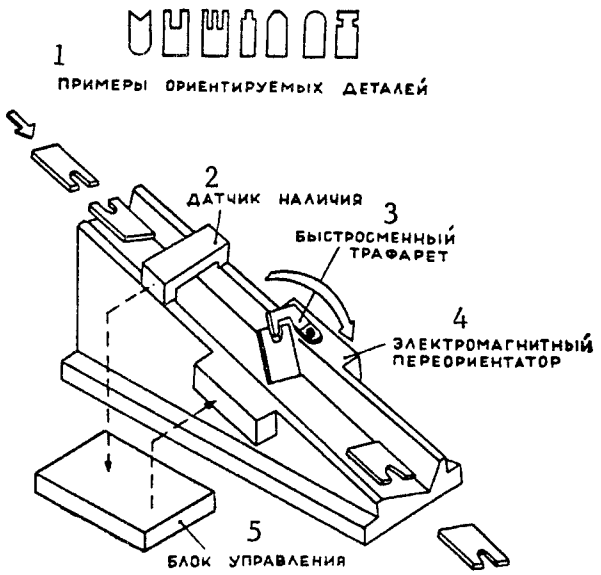

Figure 1. Universal Device for Orientation of Flat Ferromagnetic Blanks Using Elements (Notches, Projections) on the Outer Contour:

1—Examples of oriented parts; 2—Presence sensor; 3—Interchangeable pattern; 4—Electromagnetic flipper; 5—Control unit

Part position sensors (Figure 2) are used to recognize parts based on the position or shape of apertures, as well as various less obvious characteristids. If a part must be flipped, the sensor sends the instruction to switch on the electromagnetic flipper.

The throughput of an EMAGO-097 device reaches 100-150 parts per minute (depending on speed of recognizing system and power of electromagnetic flipper).

The very universal nature of electromagnetic flippers allows them to be used as actuating mechanisms in "learning" orienting devices, based on microprocessors. The device is equipped with a universal sensor and two electromagnetic flippers, allowing both longitudinal and transverse flipping of parts.

These devices are "taught" by an operator, who places parts in the recognition area in the desired position, which is then stored in control unit memory.

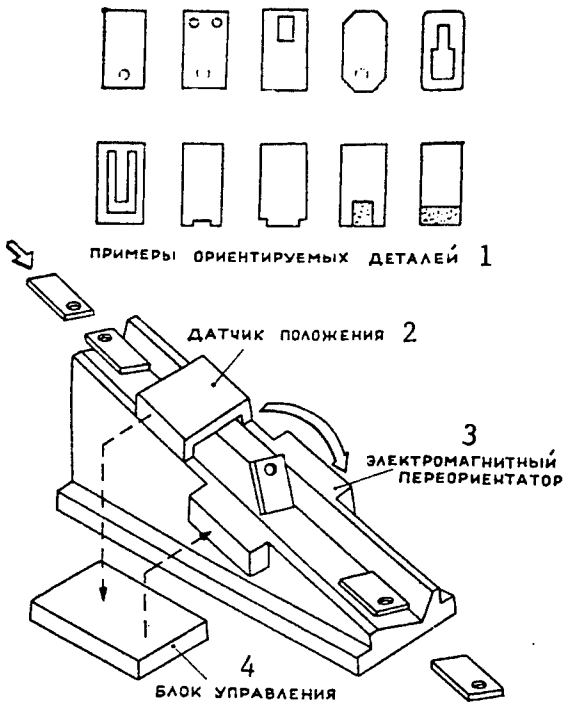

Figure 2. Device for Orientation of Flat Ferromagnetic Parts Based on Less Obvious or Concealed Characteristics:

1—Examples of parts oriented; 2—Position sensor; 3—Electromagnetic flipper; 4—Control unit

As the device operates, the recognition system compares the position of an incoming part with the position stored in memory and, if necessary, generates the commands to switch on the flippers.

The EMAGO-097 device is easily configured with loading devices (vibrating hoppers) for primary orientation and single-piece output of parts. The use of EMAGO-097 devices allows developers to avoid problems of orientation of various flat blanks and thus reduce the time required to develop forging systems.

Enterprises desiring to order the EMAGO-097 are invited to write to: 229021, Latv. SSR, Riga Rayon, Salaspils-1, Institute of Physics, Laboratory of Electromagnetic Mechanics.

Along with your letter, also send samples of the parts to be oriented (5 ea.).

Priority Topics in Research Activities of VNIITmash Scientific Production Union in Field of Die Forging Production

18420175A Moscow
KUZNECHNO-SHTAMPOVOCHNOYE PROIZVODSTVO in Russian No 4, Apr 89 (manuscript received 8 Dec 88) pp 1-3

[Introductory announcement and article by Candidate of Technical Sciences Yu.A. Sinitsyn, Deputy Director of the VNIITmash Scientific Production Union]

[Text] [introductory announcement] On April 29, 1989, the Volgograd Scientific Production Union on Machine Building Technology marks its 30th anniversary.

The VNIITmash [All-Union Scientific Research Institute on Machine Building Technology] Scientific Production Union is the main scientific technical center dealing with foundries, die forging production, and heat treatment of forgings and parts for tractors and other agricultural machinery.

The union designs new technology and perfects previously existing technology used for pressure machining of metals, thereby helping our country solve various production problems.

The editorial board and staff of this journal congratulate the union collective on its 30th anniversary and wish it further creative success.

[main article] At the Ministry of Agricultural Machinery, die-forged products take the lead in comparison to other branches of machine building in our country, both in terms of production of hot die forgings (more than 50% of their total production in the USSR) and in terms of technical and economic indices.

More than 380 automated and semiautomated production lines, machine tools and semiautomated machine tools are being used in forge shops in this branch of the industry. The output of high-quality die forgings is about 30 percent of the total output; the output of items employing parts-rolling technology is 11 percent of the total output. The following progressive technological processes are widely used: hot extrusion in solid and split dies, forge rolling of die forgings, cross taper rolling, radial expansion rolling, knurling of gear and sprocket teeth, and knurling of wheel paths and track roller flanges in tractors. More than 40 percent of the total output of hot die forgings are manufactured using a hot die forging crank press; 55 percent are manufactured using low oxidation heating.

Scientific research institutes in this branch of the industry are playing a key role in solving problems associated with improving the technical level of forging manufacture in the machine building industry, including manufacture in the field of hot die forging production.

The VNIITmash Scientific Production Union is a specialized branch institute of the Ministry of Agricultural Machinery dealing with foundries and die forging production, heat treatment, and powder metallurgy.

The institute has established the following priority topics for scientific technical research in the field of die forging production: parts-rolling technology, preshaping blanks during the forging process, flashless forging using split dies, design of automated production lines for hot coiling of springs, forging blanks using rolling combined with spinning, hot die forging using powder blanks, increasing the durability of forging dies, designing automated hopper-loading units, improving equipment used to perform heating during the forging process, improving equipment used in heat-treating furnaces.

Parts-rolling technology. Cross taper rolling is a progressive technological process for manufacturing precision forging blanks for multidiameter shafts. VNIITmash has designed the model ASK 45 and ASK 90 automated cross taper rolling mills, as well as the model K05.8440.1 automated complex. They can roll forging blanks with a diameter of 20 to 100 mm and a length of up to 630 mm. These mills ensure attainment of preset technical-economic indices and are reliable in operation. Various industry factories are using 13 of VNIITmash's mills, including the Volgograd, Chelyabinsk, and Pavlodar Tractor Factories, the Lozovskiy Mechanical Forging Factory imeni "60th Anniversary of the USSR", the Melitopol Tractor Hydraulic Unit Factory imeni "25th CPSU Congress", and the Kirovograd "Gidrosila" [Hydraulic Force] Factory. At present, cross taper rolling is used to manufacture more than 100,000 metric tons of precision forging blanks. The major advantages of cross taper rolling are: reduction of rolled metal stock consumption by 20-30 percent, increase in work productivity by a factor of 3 to 6 in comparison to hammer forging, use of hot die-forging crank presses and horizontal forging machines, and reduction of mechanical machining allowances by a factor of 1.5 to 2. The installation of a single mill results in an economic impact of about 200,000 rubles. The institute is presently working on improving the construction of cross taper rolling mills, improving their operational indices, and designing head attachments equal in quality to the best Western examples.

The institute has developed a method for simultaneously manufacturing two duck-foot shovel blades for use in cultivators and sowers. The method is based upon using a conical roll moving over a flat die to perform hot expansion rolling of the edges of the initial forging blank. An automated complex has been manufactured for expansion rolling of duck-foot shovel blades; it includes a cassette-style hopper-loading device, an induction heater, a blade expansion-rolling stand equipped with automatic feed, a feed unit, and an offloading conveyer. The cyclical output of the complex is 275 parts/hour. The complex has been installed in the "Kazakhselmash" [Kazakh Agricultural Machines] Factory imeni "50th Anniversary of the USSR".

Preshaping blanks during the forging process. The institute has designed model K500, K630, and K800 automated rolling mills, as well as complexes based upon the model K630 and K800 mills. They are designed to use a tapered tool to roll blanks with an elongated axis during small-flash hammer forging and hot die crank press forging. They are easily incorporated into hot die forging production lines. The diameter of the forging blanks being rolled is 10-90 mm; their length is up to 450 mm. By using cross taper rollers to preshape the blanks during forging, one can reduce rolled metal stock consumption by 15-20 percent and increase forging output by 20-25 percent.

Model K500 and K630 rolling mills are included in the product line of the Press-Forging Plant imeni Kalinin of the Voronezh Factory, and are manufactured to fill requisitions from various factories. At present, over 50 rolling mills have been made for the ZIL [Automobile Factory imeni Lenin] and MAZ [Minsk Automobile Factory] factories, as well as for other factories. Model K800 rolling mills have been manufactured by the experimental factory of the VNIITmash Scientific Production Union and have been installed in the Kamskiy Automobile Factory to replace mills made by the "Eumuko" firm (FRG) for use in an automated forging line for manufacture of connecting rods. Along with other types of mills, the model K800 cross taper rolling mill is used at the Lipetsk, Vladimir, and Volgograd Tractor Factories, the Lozovskiy Mechanical Forging Factory, and at other factories. The Lozovskiy Mechanical Forging Factory has incorporated the model K800 rolling mills to roll complete multidiameter axles out of tubular blanks instead of forging them on rotary swaging machines.

Flashless forging with split dies. The institute has designed automated production lines equipped with trimming presses (with a force of 4000 and 6300 kN) for use in forging "bar" type blanks having a thickened area with a complex shape on one end, e.g. tractor engine fuel-injection nozzle housings, which can be forged minus a flash by setting the blank into the face of press tools with vertically split dies. The production line output is 750 forgings per hour.

The production line used since 1982 in the Vladimir Tractor Factory operates using piece blanks made from sized hot-rolled stock cut by punches mounted on blanking presses. The blanks are loaded into the hopper of a slotted induction heater where they are heated according to zones. The forging blank is completed during the course of a single cycle. A single operator runs the production line.

A production line has been designed for the Kamyshin Forging and Casting Factory. In addition to the forging section, this line also has a blanking section. The line operates using sized cold-rolled or hot-rolled bars. An operator runs each section of the line.

In the mechanized section of a unit designed to perform flashless forging of fuel-injection nozzle housings at the Chelyabinsk Tractor Factory, the forger introduces a heated blank into the press tool and then actuates the press crosshead. The forging blank is automatically removed from the press tool; in addition, the die impression is lubricated and has compressed air blown over it automatically.

Thanks to the incorporation of automated production lines for flashless forging of fuel-injection nozzle housings, rolled metal stock consumption has dropped by 20-25 percent, work productivity has increased by a factor of 2-3, heavy manual labor has been eliminated, and capital investments have been greatly reduced (since expensive shaping equipment has been replaced with trimming presses which consume much less power).

Designing automated production lines for hot coiling of springs. Hot coiling of springs is based upon outdated equipment with low productivity and high labor expenditures. The VNIITmash Scientific Production Union has designed automated production lines for the Volgograd Tractor Parts and Standards Factory. The production lines manufacture compression springs, starting with a loading unit feeding piece blanks into the work-coil of the induction heater, and ending with the output of painted parts ready for packaging in housings (spring parameters: rod diameter 20-28 mm; outer diameter 100-150 mm; height 500-700 mm). The advantages of such lines are: they can be reset for a new spring size within a given range, they ensure production of high-quality parts, and they perform all operations during a single heating cycle. The incorporation of these lines in the Volgograd factory has increased work productivity by a factor of 3, increased the service life of springs by a factor of more than 2, greatly improved the sanitation and hygiene of working conditions, and has completely eliminated physical labor.

The institute has developed new adjustable automated production lines for hot coiling of springs in four different standard sizes for the Beloretsk Tractor Springs Factory. The new production lines employ in their design technical solutions with no equivalent in national or international practice. For example, with the aim of shortening the work cycle and ensuring high spring quality, for the very first time longitudinal rolling has been replaced with the following: cross taper rolling of the ends of the blank with simultaneous cutting of both ends to size, use of a machine generator with a 66 kHz frequency for additional heating of rods with a diameter of up to 20 mm, and simultaneous grinding of the two ends of the spring via rotational movement and oscillation of the spring.

Forging blanks using rolling combined with spinning. There is special interest in using deformation caused by local loading, and in particular in using rolling combined with spinning during forging. The VNIITmash Scientific Production Union has been dealing with this topic for about 10 years. The institute has designed an experimental hot-stamping press which (in terms of its structural solutions and technological capabilities) is in no

way inferior to the best presses made by the Massey (England) and Schmid (Switzerland) Companies.

The major advantages this experimental press has over its foreign equivalents is its ability to combine rolling/spinning forging with simultaneous extrusion of a central cavity; it can also combine rolling/spinning with torsional processes. The nominal pressing force is 2000 kN; there are 900 oscillations per minute; the maximum diameter of the blank being forged is 200 mm.

The creation of this press was preceded by the design of rolling/spinning attachments and end-face expansion attachments, as well as various technological processes involving forging using the rolling/spinning process. Among the processes which have found widest practical applications, we may single out the use of the rolling/spinning process to forge:

1) ring-shaped parts (e.g. the rings of hydraulic hitches) made from rod-type blanks which have been previously bent into rings—their use at the Volgograd and Pavlodar Tractor Factory Production Unions made it possible to reduce average rolled metal stock expenditures by a factor of 2.8, while labor expenditures for manufacturing parts were reduced by a factor of 1.5;

2) bimetallic pistons for the 8DVT-330 diesel engine for the Chelyabinsk Tractor Factory Production Union. Using the rolling/spinning process to forge steel and cast iron ring mounts onto these pistons made it possible to obtain a stable depth, a set tightness of fit for the piston, a sealed combustion chamber surface structure, and (as a result of this) an increase in the engine service life several times over.

Hot forging of powder blanks. Since 1985 the VNIITmash Scientific Production Union has been a part of the Interdepartmental Scientific Technical Committee on "Powder Metallurgy." The institute has worked in tandem with design organizations and enterprises in the industry to develop a range of products with the aim of basing their manufacture upon hot-forged powder materials. High-density parts have been manufactured which operate under heavy load conditions and which have high precision and a metal utilization factor of more than 0.8. The institute has worked along with the Vladimir Tractor Factory Production Union to perform experiments on selecting material and developing a technology for using hot forging of powders to manufacture hydraulic hitch joints, transmission forks, control levers, and spline sleeves. These parts have been tested for serviceability and have produced positive results. The Vladimir and Pavlodar Tractor Factory Production Unions plan to incorporate this technology.

A technology has been developed for using hot forging of powder blanks to manufacture connecting rods used in the PD10U and P350 starting engines. Experiments have shown that this type of connecting rod ensures a starting engine service life sufficient for 8,000 hours of main engine operation.

The Vladimir and Chelyabinsk Tractor Factory Production Unions joined the UkSSR Academy of Sciences Institute on Problems in Mechanics in order to develop a technology for using hot forging of powder blanks to manufacture packing rings used in standard end-face seals found in the moving sections of industrial and agricultural tractors. The scientific production union of the State Union Research Institute on Tractors performed experiments which showed that the new rings ensure a seal service life of more than 10,000 hours of engine operation for agricultural tractors, and more than 6,000 hours of engine operation for industrial tractors. This greatly exceeds the hours of engine operation for rings manufactured from steel type ShKh15. The production union of the Vladimir Tractor Factory performed industrial testing on this technology. Experiments are being carried out on using metallic powders to manufacture packing rings at the Kremenets Metallic Powder Parts Production Factory.

Increasing durability of forging dies. The institute has performed a great deal of work on increasing the durability of forging dies. One progressive technological process is to produce the cast blanks for forging dies via electroslag refining (ESR), where worn-out dies act as the consumable electrodes. The ESR process makes it possible to create a new alloy in forging dies made out of steel types 5KhNM, 5KhNV, 5KhNT, and 4KhMFS via the introduction of composite electrodes, with the addition of wastes from machine-tool manufacture. Thanks to the improvement in metal quality, the die durability increases by 30-40 percent. Six ESR installations have been incorporated into factories in this branch of the industry, following the designs proposed by VNIITmash.

The durability of forging dies has also been increased by using new types of forging steels. The institute has developed a new type of forging steel called 4KhM2Fch for manufacture of inserts used in hot die-forging crank presses and horizontal forging machines. The "Krasnyi oktyabr" [Red October] Volgograd Metallurgical Factory produces this steel in the form of rolled stock with a diameter of 80-250 mm. The durability of forging dies made from steel 4KhM2Fch is 1.5-2 times greater than the durability of dies made from steel 4KhMFS.

The model UNF-6M machine has been introduced into 20 factories in this branch of the industry and in other machine building ministries. This machine has a phototracking system which follows drawings/templates, automatically facing trimming dies under a flux. The use of automatic facing allows one to replace expensive tool steel with carbon steel 45, increasing (by a factor of 3) the durability of dies faced with wire made from steel sv20Kh13. Heat treatment is not required after facing—the dies are immediately subjected to grinding and electric pulse machining.

Designing automated hopper-loading units. The institute has designed and manufactures (up to 50 units per year) automated loading complexes in two standard sizes intended to automate the loading of cylindrical and

cubical blanks into the induction heater used in forge shops. The greatest length for blanks which can be loaded is 300 mm at a diameter of 15-100 mm (first standard size) or 400 mm at a diameter of 70-150 mm (second standard size).

The complex consists of a metering loader, a disk-shaped orientator, a control panel, and several sensors. The disk-shaped orientator ensures reliable orientation of the blanks applied to its bowl in portions of up to 400 kg; it also uses feed rollers to ensure pressure feed of the blanks.

The complex has the following advantages: it can be quickly readjusted for various standard blank sizes; it has high operational reliability as blanks are loaded into it after being cut using standard press-shears; it can perform many operations—hopper loading, orientation, and pressure feed of blanks through the induction heater work-coil at a set speed (including the final blanks in a portion); its noise level is no greater than 50 dB; it has a relatively small power consumption.

Improving equipment used to perform heating during the forging process and equipment used in heat-treating furnaces. The "Teploagregat" [Heat Assembly] Special Technological Design Office (part of the VNIITmash Scientific Production Union) has been performing scientific research on improving equipment used to perform heating of blanks during the forging process and equipment used to heat-treat forgings. Recently, specialists in this office have: developed new gas heating furnaces in 18 standard sizes for the Vladimir Tractor Factory Production Union; finished 16 recuperative heat exchanger projects, including spray, radiation, and double-circulation (one pipe within another pipe) types; developed three types (KGMG-A, GKVG, and GKHD) of burners intended for preheated blast-air applications; and have developed hardening-tempering assemblies, assemblies for isothermal annealing of forgings, and a two-stage assembly for normalizing forgings.

A number of the aforementioned topics have resulted in the development of specific complex industrial programs for the 12th 5-year plan. Once realized, these programs will ensure further improvement in the technological level of die forging production in this branch of the industry.

UDC 621.3.049.776.535.37

Anodic Oxidation of Film on Aluminum Alloyed With Rare-Earth Metals

18420188A Minsk VESTSI AKADEMII NAVUK BSSR: SERIYA FIZIKO-TEKNICHNYKH NAVUK in Russian No 1, Jan-Mar 89 (Manuscript received 17 Nov 87) pp 106-108

[Article by V. A. Sokol, M. M. Pinayeva, G. P. Lavrik, A. P. Kovarskiy, Minsk Institute of Electronic Engineering]

[Text] One method of improving the properties of anodic oxide films is to alloy them. Rare-earth metals have been suggested as additives in the process of producing thin films to improve their stability and resistance to electric diffusion[1, 2]. It has been shown that introduction of rare-earth metal oxides to Al_2O_3 film can improve adhesion to the substrate and increase the dielectric strength of films by a factor of 2-2.5.

In this article we present the results of investigation of anodic oxide films produced by anodization in an aqueous solution of citric acid. The rare-earth metals were introduced to the anodic oxide films from an electrolyte in the process of anodization.

Method of investigation

Films of aluminum 0.5-0.8 μm were dusted onto pyroceram substrates type ST-50-1 by electronic heating of a crucible on an UVN-74P-3 installation. The anodic oxide films containing rare-earth metals (Nd, Gd, Eu, Ho, Er, Tu, Lu) were obtained with a type P-5872M potentiostat in a combined mode with constant scanning of the voltage at 1 V/s in an electrolyte based on an aqueous citric acid solution containing a complex rare-earth metal compound, dissociated in the electrolyte to form a complex rare-earth metal anion. The penetrating anodic oxidation voltage was 135 V, current density 1 mA/cm^2, residual current density not over 3% of the maximum current density.

Experimental Results and Their Discussion

The luminescence method previously suggested by us[3] was used to study the mobility of the complex rare-earth metal anion. It is based on the ability of certain rare-earth metals to cause scintillation in the visible area when struck by ultraviolet light. Of greatest interest in this respect is europium, which has intense luminescence in the red area (around 580-640 nm). The luminescence spectrum of the Eu^{3+} ion is convenient due to the simplicity of its interpretation.

Figure 1 shows the luminescence spectrum of the Eu^{3+} ion in the reagent Eu_2O_3 (1) and in an electrolyte containing the complex europium anion (2). The Eu^{3+} ion in Eu_2O_3 yields a bright red visual glow, whereas in the electrolyte it has a muddy pink glow of very low intensity, which, in combination with the results of analysis of the structure of electron transitions in spectra (1) and (2), unambiguously indicates inclusion of the Eu^{3+} ion in a complex compound in the internal coordination sphere.

The luminescence spectra of the Eu^{3+} ion, recorded from the surface of an anodic oxide film under identical conditions in the 580-640 nm area (Figure 1.3) do not have linear structure, indicating the amorphous state of the films. Anodic oxide films obtained in an electrolyte with pH=3.15-4.0 had a clear visible red glow. This indicates the presence of the Eu^{3+} ion in the anodic oxide film in cation form. The values of total luminescence intensity of the Eu^{3+} ion in anodic oxide films at pH=2-4

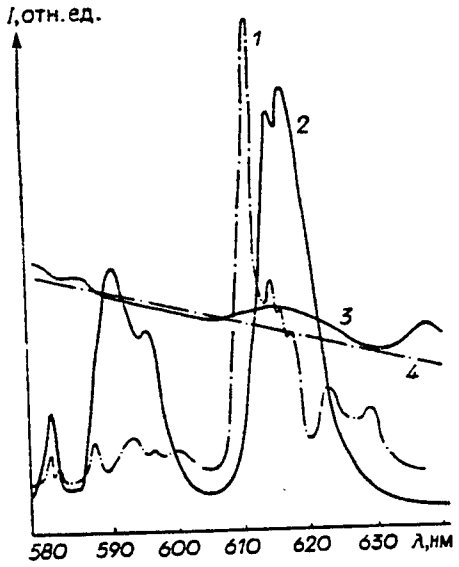

Figure 1. Luminescence Spectra of Eu^{3+} Ion:
Key: 1—Reagent Eu^2O^2; 2—Electrolyte containing complex europium anion; 3—Surfaces of anodic oxide films alloyed with europium; 4—Background line for (3)

were as follows:

pH	2.0	2.5	3.0	3.15	3.5	4.0
I, rel. units	0	0	18.2	43.7	49.1	51.3

As we can see from the data presented, increasing the pH of the electrolyte helps to increase the mobility of the complex europium anion in an electrolyte.

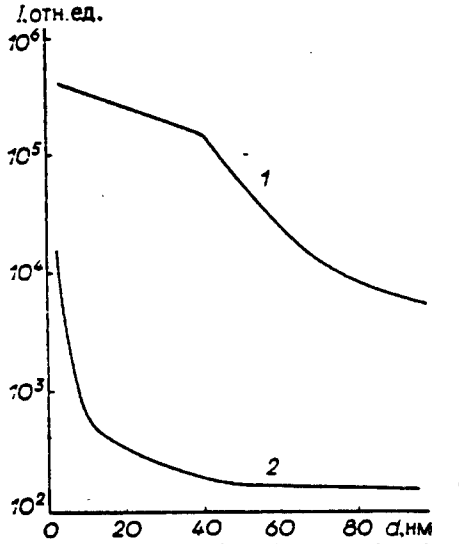

Figure 2. Distribution Profile of Neodymium in Anodic Oxide Film:
Key: 1—AlO^+_2 = 2—Nd^+

We studied the electrolyte anion element distribution profile in anodic oxide films by the method of secondary ion mass spectrometry. Figure 2 shows the distribution profile of neodymium in an anodic oxide film (it is similar for the other rare-earth metals). As we can see from the figure, the content of neodymium in the anodic oxide film surface is maximal, indicating high mobility of its complex anion in the electrolyte (pH=3.2). Howver, as we move into the depth of the anodic oxide film, the content of neodymium decreases and at a depth of about 10 mm it drops by 1.5 orders of magnitude then regularly and uniformly decreases to the interface between the anodic oxide film and the metallic aluminum.

Thin-film condensors were produced in order to determine the electrophysical parameters of anodic oxide films containing rare-earth metals. Capacitance was measured on a type MTsE-15A instrument.

The table presents the electrophysical parameters of thin-film condensors with a dielectric containing gadolium, holmium, erbium, thulium and lutecium. The insulation resistance in all cases with a voltage of +50 V was 10^{11} Ohms, with a voltage of -50 V—10^{10} Ohms. The specific capacitances were averaged for three batches studied. The yield of good products in all cases was close to 100%.

Analysis of the results in the table indicates that the capacitance of thin-film condensors increases slightly in the sequence of the rare-earth metals.

Comparison of the electrophysical parameters of thin-film condensors with thin-film condensors using a dieletric based on Al_2O_3, produced in a 1% solution of citric acid, shows that in this case tan δ decreases by a factor of about two, while leakage current decreases by an order of magnitude and, which is particularly important, the yield of good condensors is almost 100%. Obviously, a more detailed study of the structure and properties of anodic oxide films containing rare-earth metals from an electrolyte is required to explain the results obtained. However, the improvement in electrophysical parameters of thin-film condensors indicates first of all a decrease in the defect content of the dielectric layer, particularly a decrease in the number of microscopic pores, channels with reduced dielectric strength, and degree of crystallinity[5].

References:

1. Dzhuplin, V. N., Zaichkin, N. N., Krasnikh, S. A., Chistyakov, Yu. D., Elektronnaya Tekhnika [Electronic Equipment], Microelectronics Series, 1977, No. 1 (67), p 95.

2. Koleshko, V. M., Belitskiy, V. F., Massoperenos Na Tonkikh Plenkakh [Mass Transfer in Thin Films], Minsk, 1980.

3. Labunov, V. A., Sokol, V. A., Pinayeva, M. M., et al., Dokl. AN BSSR, 1984, Vol. 28, No. 3, pp 215-217.

4. Sokol, V. A., Pinayeva, M. M., Vorobyeva, A. I., Chekalova, I. I., Elektronnaya Tekhnika [Electronic Equipment], Materials Series,, 1985, No. 7 (206), p 53.

5. Golubkova, V. I., Kotousova, I. S., Paverko, Ye. I., Mirzoyev, R. A., Elektronnaya Tekhnika [Electronic Equipment], Radio Parts and Components Series, 1979, No. 5 (36), pp 16-27.

1 Исследованная партия	2 Гадолиний		3 Гольмий		4 Эрбий		5 Тулий		6 Лютеций	
	$C_{уд} \cdot 10^{-8}$, Ф/м²	tgδ, %	$C_{уд} \cdot 10^{-8}$, Ф/м²	tgδ, %	$C_{уд} \cdot 10^{-8}$, Ф/м²	tgδ, %	$C_{уд} \cdot 10^{-8}$, Ф/м²	tgδ, %	$C_{уд} \cdot 10^{-8}$, Ф/м²	tgδ, %
1	37,2	0,50	41,7	0,47	39,5	0,49	39,9	0,47	42,0	0,48
2	42,0	0,48	41,2	0,47	41,8	0,49	41,8	0,47	41,8	0,49
3	41,1	0,47	41,8	0,49	41,0	0,49	42,1	0,50	41,6	0,50
7 Среднее значение	40,1	0,48	41,6	0,48	40,8	0,49	41,3	0,48	41,8	0,49

Electrophysical Parameters of Thin- Film Condensors with Dielectric Containing rare-earth metal
Key: 1—Group studied; 2—Gadolinium; 3—Holmium; 4—Erbium; 5—Thulium; 6—Lutecium; 7—Mean value

UDC 621.382(088.8)

Influence of Conditions of Formation of MOS Structures on Charge Captured in Oxide Under External Forces

18420188B Minsk VESTSI AKADEMII NAVUK BSSR: SERYYA FIZIKA-TEKNICHNYKH NAVUK in Russian No 1, Jan-Mar 89 (Manuscript received 19 Jan 88) pp 108-111

[Article by N. V. Rumak, V. V. Khatko, V. P. Apanacenko, A. M. Aliyev, Institute of Physics and Technology, Belorussian Academy of Sciences]

[Text] When ionizing radiation acts on an MOS structure, both the density of surface states at the silicon-oxide interface, and the positive charge in the SiO_2 change[1], leading to an increase in the slope and offset of the volt-farad characterisics found in C-V-method studies. It is interesting to investigate the influence of formation conditions of a gate dielectric and field electrode on the change in parameters of MOS compositions under external influences, since the available experimental data[2-4] are insufficient for prediction of the characteristics of structures manufactured considering present-day trends in solid-state microelectronics.

Metal-oxide-semiconductor structures were created by thermal oxidation of electron-type silicon in atmospheres of Ar-O_2-HCl and H_2-O_2-HCl. The thickness of silicon dioxide films was 15-40 nm, for which the greatest changes in structure and electrophysical properties of the oxides are observed[5]. The field electrodes were alloys of aluminum with silicon and molybdenum 300 nm thick, applied by the electron-beam and magnetron methods.

Structures with positive bias on the electrode (E=1.25 $mV \cdot cm^{-1}$) were exposed to x-ray radiation from tubes with molybdenum (λ_{Mo}=0.071 nm) or chromium (λ_{Cr}=0.229 nm) anodes on a series-produced URS-2.0 installation, and the results were compared with data for specimens exposed to γ radiation from a ^{60}Co source with an exposure dose of $3 \cdot 10^2$ rad/s. The absorption dose in the gate dielectric with x-radiation was computed by the method of[6] from the volt-ampere characteristics measured with the external influence. The rates of dose accumulation computed from these data were $7.9 \cdot 10^4$ (λ_{Mo}) and $11.8 \cdot 10^4$ (λ_{Cr}) rad/s. The high values of dose rate for x-radiation were related to the specifics of the radiation geometry, the finite dimensions of the source and possible "leakage" of the charge beneath the electrode during measurements. The result of exposure of the MOS structure to ionizing radiation were evaluated on the basis of the change in inversion voltage (ΔU_{inv}), the value of which is determined by the total charge density captured in oxide boundary- layer traps and in

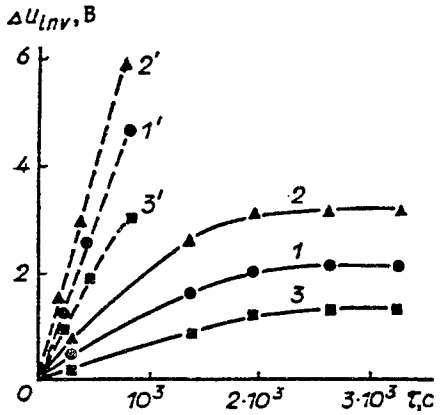

Figure 1. Change in MOS-Structure Inversion Voltage for Structures with Dry Oxide 40 nm Thick As a Function of Time of Exposure to Gamma- (1, 2, 3) and X-Ray (1', 2', 3') Radiation;

Key: 1, 1' and 2, 2'—Specimens with Aluminum Electrodes Applied by Magnetron and Electron-Beam Methods; 3, 3'—Specimens with Molybdenum Electrode Applied by Magnetron Atomization

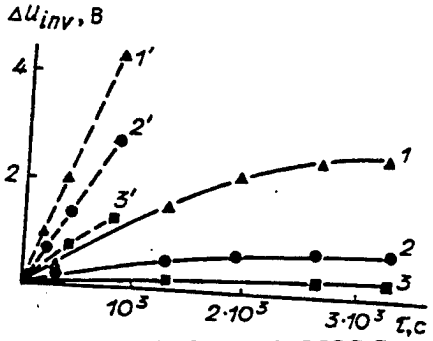

Figure 2. Variation in Change in MOS-Structure Inversion Voltage for Structures with Pyrogenous Oxide As a Function of Time of Exposure to Gamma- (1, 2, 3) and X- Ray (1', 2', 3') Radiation;
Key: 1, 1' and 2, 2'—Specimens with Aluminum Electrodes Applied by Electron-Beam Method to Oxide 40 and 30 nm Thick; 3, 3'—Specimens with Molybdenum Electrode Applied by Magnetron Method to Oxide 40 nm Thick

surface states at the semiconductor-dielectric interface. The inversion voltage (U_{inv}) of the specimens was found from the high-frequency volt-farad characeristics, recorded at 1 MHz.

Figures 1 and 2 show the time variations of ΔU_{inv} for MOS structures with gate dielectric obtained in atmospheres of Ar-O_2-HCl (dry "oxide") and H_2-O_2-HCl ("pyrogenous" oxide). We can see that the different types of ionizing radiation have a different influence on the measured values of U_{inv} of the specimens studied: γ radiation causes its saturation after a time while x-radiation does not cause saturation. This is a result of the influence of dose rise rate and the varying contribution of surface states to ΔU_{inv} in the two cases (Figure 3).

Analysis of the influence of the silicon oxidation atmosphere and thickness of the gate dielectric on the charge captured in the MOS structure oxide during external influences indicates that for the pyrogenous oxide the increase in ΔU_{inv} is characteristically less than for the

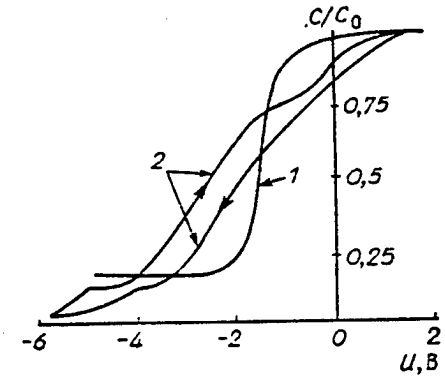

Figure 3. Form of Volt-Farad Characteristics After - (1) and X-Ray (2) Radiation

dry oxide, and with increasing oxide thickness it is retarded. The smallest value of ΔU_{inv} in the saturating mode was found in specimens with dielectric 15 nm thick. This tendency toward changing inversion voltage with a decrease in gate dielectric thickness is known [7]. It is usually related to a decrease in the volume of the material. However, this approach is insufficient, since it does not allow us to explain the influence of the type of oxidizing atmosphere on the stability of the properties of the dielectric.

To interpret the results produced, we assumed that the basic source of additional positive charge in the oxide might be excess atoms of silicon or other impurity atoms. The films of silicon dioxide, grown in dry and moist atmospheres, have different degrees of microporosity, the value of which is higher in the latter case[5] and increases with decreasing oxide thickness. An increase in microporosity facilitates the removal of excess silicon atoms from the SiO_2 transition area. This process is activated by the presence of hydrogen in the oxidizing atmosphere, facilitating transfer of silicon atoms from micropores into the gas stream. Thus, the decrease in the value of ΔU_{inv} for specimens with pyrogenous oxide and with thinner oxide films should be related to the decrease in the content of excess silicon atoms at the Si-SiO_2 interface.

The influence of electrode type and method of its application on the change in MOS structures under external influences is determined by the level of macrostresses in the SiO_2 transition layer and possible diffusion of particles from the metal to the oxide.

We know that the process of electron-beam application of aluminum films stimulates the transfer of aluminum particles and impurities into the gate dielectric. This can explain the maximum level of ΔU_{inv} in MOS structures made by electron-beam atomization. The offset of the volt-farad characteristics of these specimens resulting from x-radiation is determined primarily by the increase in the density of induced surface states. However, the use of the magnetron method of application of metal films, causing an increase in great compressive macrostresses (both static and dynamic) in the SiO_2 transition layer near the Si-SiO_2 interface, helps to increase the stability of the inversion voltage under external influences. This effect is based on the crystallization of the oxide in microscopic volumes of the boundary layer, containing excess silicon atoms, under the influence of macrostresses and impurity modifiers (including excess silicon), which is accompanied by ionization of impurity modifiers in the field of elastic forces of the crystalline seed lattice[5]. Consequently, the presence of these impurities in the oxide does not influence the change in inversion voltage with external influences, since the probability of secondary ionization is slight.

For comparison, Figures 1 and 2 show data for structures with polysilicon field electrode. The greatest change in inversion voltage with external influences is characteristic for specimens with dry oxide. This is related to the

significant increase in the charge captured on surface states of the division boundary. For MOS structures with pyrogenous oxide, the change in U_{inv} is comparable to the data for specimens with metal electrodes.

Thus, the creation of MOS structures can be controlled by changing the inversion voltage by ionizing radiation. This is primarily related to the decrease in concentration of excess silicon atoms and other impurity modifiers in the transition area of the silicon dioxide near the semiconductor-dielectric interface by selecting suitable technological processes.

References:

1. Z and S., Fizika Poluprovodnikovykh Priborov [Physics of Semiconductor Devices], Moscow, 1984, Vol. 1, 456 pp.

2. Popov, V. D., Radiatsionnaya Fizika Priborov So Struktyuroy Metall-Dielektrik-Poluprovodnik [Radiation Physics of Devices with Metal-Dielectric-Semiconductor Structure], Moscow, 1984.

3. Astvyatsaturyan, V. R., Belyaev, V. A., Zaytsev, V. L., Zarubezhnaya Elektronnaya Tekhnika, 1986, No. 2, pp 62-99.

4. Chernyshev, A. A., chepizhenko, A. Z., Borisov, Yu. A., et al., Zarubezhnaya Elektronnaya Tekhnika, 1986, No. 7, pp 3-157.

5. Rumak, N. V., Sistema Kremniy-Dvuokis Kremniya Va MOP- Strukturakh [The Silicon-Silicon Dioxide System in MOS Structures], Minsk, 1986.

6. Snow, E. H., Grouv, A. C., Fitzgerald, D. I., Proc. IEEE, 1967, Vol 55, No 7, pp 1168-1185.

7. Shiono, N., Shimaya, M., Sano, K., Jap. J. Appl. Phys., 1983, Vol. 22, No. 9, pp 1430-1435.

UDC 669.017.2:621.785.16

Recrystallization of Deformed TS6 Titanium Alloy With Rapid Continuous Heating

18420188C Minsk VESTSI AKADEMII NAVUK BSSR: SERYYA FIZIKA-TEKNICHNYKH NAVUK in Russian No 1, Jan-Mar 89 (Manuscript received 1 Dec 87, deposited in VINITI 13 Jan 88) p 112

[Abstract of article by A. I. Gordienko, V. V. Ivashko, R. S. Novik, Institute of Physics and Technology, Belorussian Academy of Sciences]

[Text] A study is made of the kinetics of recrystallization and grain growth in hot- and cold-deformed sheets of TS6 alloy upon heating at 10-100 °C/s. It is shown that in hot-deformed sheets recrystallization is completed at 1100-1200°C, grain size 80 μm. In cold deformed sheets with 50% compression heated at 10 and 100°C/s, recrystallization is completed at 850 and 1075°C, and primary recrystallized grain size is 35-40 μm. References 7.

UDC 621.436-462:006.354

Valve Tappet: Conditions of Operation and Material Selection

18420188D Minsk VESTSI AKADEMII NAVUK BSSR: SERYYA FIZIKA-TEKNICHNYKH NAVUK in Russian No 1, Jan-Mar 89 (Manuscript received 10 Feb 87; deposited at VINITI 16 Apr 87) p 112

[Abstract of article by L. R. Dudetskaya, Yu. T. Antonishin, A. I. Pokrovskiy, Institute of Physics and Technology, Belorussian Academy of Sciences]

[Text] The operating conditions of an internal combustion engine valve tappet are studied. It is shown that the working surface of the tappet is subjected to high contact loads, while the temperature in some areas may exceed the critical points of phase transformations for the tappet material. The structural changes occurring under these conditions cause loss of strength and rapid wear. The nature of these changes in various stages of operation and the mechanism of the strength loss and wear are described.

Requirements are formulated which must be satisfied by the structure and properties of the tappet material. Materials used at the present time are analyzed. The advantages of alloyed cast iron, containing martensite and a ledeburite eutectic are demonstrated. References 26.

UDC 669.295.5:621.785

Hardening of Titanium Alloys and Medium-Carbon Structural Steels by Electric and Electron-Beam Heating

18420188E Minsk VESTSI AKADEMII NAVUK BSSR: SERYYA FIZIKA-TEKNICHNYKH NAVUK in Russian No 1, Jan-Mar 89 (Manuscript received 23 Oct 87; deposited at VINITI 11 Nov 87) p 113

[Abstract of article by A. A. Shipko]

[Text] Surface electron-beam hardening of titanium alloys forms a hardened layer 1-3 mm thick with phase composition which varies through its thickness and grain size from 100-200 μm to the initial grain size. When α'-martensite is present in the structure, fractures of the alloy have a tough, pitted structure with "feathered" microrelief. Fracture of the primary α phase occurs both by viscous shear and by separation of particles with conservation of depressions.

Electrochemical heat treatment can significantly reduce the processing time, achieving compact layers of chemical compounds up to 20 μm thick with a solid solution zone beneath them. This method can solve the problem of hardening heavily loaded steel parts (rapid carbonitriding), but for titanium alloys, which form small-volume stable chemical compounds with extended areas of homogeneity, it is impossible to form sufficiently

thick diffusion layers. When copper, iron and nickel galvanic coatings are used with subsequent oxidation, siliciding, nitriding or carburizing, the thickness of the wear-resistant layer is increased to 1 mm.

Wear resistance can be increased by two to three times, the bond strength of galvanic and gas-thermic coatings on titanium alloys can be increased to 200-210 MPa by electron-beam and induction heating. Characteristic stages of the process (recrystallization of chromium, diffusion through the titanium β-grain boundaries, recrystallization after melting, the sequence of eutectic reactions through the layer thickness, etc.) are recorded and studied, which would be impossible with slow heating. The distribution of elements in the transition zone is noted for electron beam heating of rutile and nickel-titanium coatings, including with melting of the coating and substrate. References 8.

UDC 621.9.02-589.22

Rotation Cutting of Wear-Resistant Powder Coatings

18420188F Minsk VESTSI AKADEMII NAVUK BSSR: SERYYA FIZIKA-TEKNICHNYKH NAVUK in Russian No 1, Jan-Mar 89 (Manuscript received 25 Jan 88; deposited at VINITI 25 Feb 88) p 113-114

[Abstract of article by P. I. Yashcheritsyn, A. V. Borisenko, I. G. Drivotin, Institute of Physics and Technology, Belorussian Academy of Sciences]

[Text] The effectiveness is shown of using the method of rotation cutting to work parts with hardened wear-resistant coatings of self-fluxing PG-SR2 and PG-SR3 powders with hardness up to 48 HRC_e. Results are presented from studies of the process of rotation cutting of wear-resistant powder coatings, the design of a rotation cutter for processing of difficultly workable powder coatings is described, as well as an original single-rotation tool holder and a device for sharpening rotation cutting tools. Recommendations are given for the use of rotation cutting tools to work parts with hardened wear-resistant powder coatings to increase tool life, improve the quality of worked surfaces and increase the productivity of working. References 2.

UDC 517.92:536.42+621.365.3

Computation of Electric-Contact Heating Parameters Considering Heat Transfer by Convection and Radiation

18420188G Minsk VESTSI AKADEMII NAVUK BSSR: SERYYA FIZIKA-TEKNICHNYKH NAVUK in Russian No 1, Jan-Mar 89 (Manuscript received 29 Jan 88; deposited at VINITI 25 Feb 88) p 114

[Abstract of article by V. V. Klubovich, V. V. Rubanik, A. A. Yakhnovets, Vitebsk Department, Institute of Solid State Physics and Semiconductors, Belorussian Academy of Sciences]

[Text] A study is made of a mathematical model of electric- contact heating by a moving wire. A differential equation is produced based on the balance of enery applied and lost, ignoring heat conductivity. A nonassociative induced algebra method is used to obtain the solution in the form of an exponential series, the coefficients of which depend on the heating parameters. Limiting the analysis to three terms of the series, the variation in current as a function of wire dimensions, physical characteristics of the metal and technological parameters of the process is found. The divergence between experimental and calculated data is not over 15-20%. References 9.

UDC 621.778:621.785

Thermoultrasonic Annealing of Steel Wire

18420188H Minsk VESTSI AKADEMII NAVUK BSSR: SERYYA FIZIKA-TEKNICHNYKH NAVUK in Russian No 1, Jan-Mar 89 (Manuscript received 29 Jan 88; deposited at VINITI 25 Feb 88) p 114

[Abstract of article by V. V. Klubovich, V. V. Rubanik, Yu.V. Tsarenko, Vitebsk Department, Institute of Solid State Physics and Semiconductors, Belorussian Academy of Sciences]

[Text] A method is described for rapid electric-contact annealing of steel wire with superimposed ultrasonic oscillations.

Results are presented from studies of the mechanical properties of the wire as a function of the annealing rate, annealing temperature and cooling conditions. It is demonstrated that the optimal annealing temperature of the steel wire decreases when ultrasonic oscillations are used, the microstructure of the steel contains a large quantity of ferrite, pearlite and ferrite particles are distributed more uniformly through the volume of the metal. References 8.

UDC 621.9.048.4

Conditions for Hardening Worked Surface in Electroerosion Grinding

18420188I Minsk VESTSI AKADEMII NAVUK BSSR: SERYYA FIZIKA-TEKNICHNYKH NAVUK in Russian No 1, Jan-Mar 89 (Manuscript received 4 Dec 87; deposited at VINITI 13 Jan 88) p 115

[Abstract of article by I. D. Shirokanov, Institute of Physics and Technology, Belorussian Academy of Sciences]

[Text] Results are presented from studies of the hardening of surfaces worked by electroerosion grinding. It is established that with a large quantity of gas-vapor phase in the interelectrode gap, dicharge conditions arise under which a layer of metal with high wear resistance is formed on the worked surface.

Based on the experimental data and theoretical conclusions, equations are derived for determination of the rate of filling of the interelectrode gap with the gas-vapor phase.

As a result of the studies performed, a relationship is established between the required rate of motion of the electroerosion tool and the parameters of the pulsed discharge, producing optimal results in terms of rate of metal removal and surface hardening.

UDC 621.793

Theoretical Estimate of Axial Temperature and Atomization Distance in Gas-Thermal Application of Coatings

18420188J Minsk VESTSI AKADEMII NAVUK BSSR: SERYYA FIZIKA-TEKNICHNYKH NAVUK in Russian No 1 Jan-Mar 89 (Manuscript received 28 Jan 88; deposited at VINITI 25 Feb 88) p 115

[Abstract of article by N. N. Dorozhkin, T. M. Abramovich, V. K. Yaroshevich, O. L. Ravun, Belorussian Polytechnical Institute]

[Text] Experimental and theoretical studies are performed of the processes occurring in the two-phase stream of gas and powder particles during gas-thermal application of coatings.

Based on the theory of a submerged turbulent jet, an expression is produced to determine the gas temperature along the axis of the stream, which agrees satisfactorily with experimental data on gas- flame atomization. Assuming that Bi is much less than one (Bi is the Biot number), equations are derived to estimae the time required to heat powder particles to the melting point and to melt them in the initial stream section, and calculation equations are produced for the atomization distance. The results obtained for heat-transfer time agree satisfactorily with experimental data. References 13.

UDC 621.824.3:539.4.012

Calculation of Load on Crankshafts Considering Their Operation in Engines

18420188K Minsk VESTSI AKADEMII NAVUK BSSR: SERYYA FIZIKA-TEKNICHNYKH NAVUK in Russian No 1, Jan-Mar 89 (Manuscript received 29 Dec 87; deposited at VINITI 25 Feb 88) p 116

[Abstract of article by M. S. Yankevich, Institute of Problems of Reliability and Durability of Machines, Belorussian Academy of Sciences]

[Text] The loads on crankshaft bearings are calculated, considering the specifics of their operation in engines.

We know that as an engine operates, the crankshaft is continually flexed due to settling of the bearings. This moves the sections of load application both in the connecting-rod bearings and in the main bearings. This is considered in the detemination of compliance factors in determining the angles of rotation of the reference sections.

The equations here presented can significantly expand the capabilities for analysis of the loading of crankshafts under realistic operating conditions.

The general form of the resulting system of equations for calculation of external loads acting on a structure is distinguished by its novelty and is effective for use with computers. References 8

UDC 621.71.927.5

Use of Follow Gas Flow in Arc Surfacing With Gas-Powder Jet

18420188L Minsk VESTSI AKADEMII NAVUK BSSR: SERYYA FIZIKA-TEKNICHNYKH NAVUK in Russian No 1, Jan-Mar 89 (Manuscript received 13 Oct 87; deposited at VINITI 11 Nov 87) p 116

[Abstract of article by N. N. Dorozhkin, N. N. Petyushev, Institute of Problems of Reliability and Durability of Machines, Belorussian Academy of Sciences]

[Text] A description is presented of arc surfacing with a powder surfacing material fed into the welding bath in a two-phase jet in the gas follow stream. The use of the follow stream surrounding the gas-powder jet decreases the loss of powder, stabilizes powder feed, allows the introduction of a powder additive to the desired area of the preliminarily formed liquid metal layer. Expressions are produced which describe the change in dimensions of the powder input zone as a function of the ratio of speed of the stream to jet velocity m. It is found that the minimum entry zone is achieved where m is between 0.8 and 1.1. In the range of m from 0.5 to 0.8, the nozzle may be located at a distance from the arc which guarantees protection of its exit aperture from electrode metal spray. References 2.

UDC 621.833.6

Method of Synthesis and Algorithm for Determination of Parameters of Differential Shaft-Planetary Transmissions

18420188M Minsk VESTSI AKADEMII NAVUK BSSR: SERYYA FIZIKA-TEKNICHNYKH NAVUK in Russian No 1, Jan-Mar 89 (Manuscript received 9 Mar 88; deposited at VINITI 13 Apr 88) p 117

[Abstract of article by V. N. Shakolin, V. N. Stukachev, A. A. Platonov, Institute of Problems of Reliability and Durability of Machines, Belorussian Academy of Sciences]

[Text] A method is presented for synthesis of differential shaft-planetary transmissions based on analysis of their structure and gear plans. Kinematic diagrams are presented for a family of shaft-planetary transmissions

including coaxial and noncoaxial models, constructed according to the method suggested. A method and algorithm are presented for computing the parameters of the transmissions as functions of the required distribution of transfer numbers. Results are presented from calculations using a program which runs on an elektronika D3-28 microcomputer. References 7.

UDC 678.621.317.738

Computation of Electric Field Strength and Capacitance of Sensor for Measurement of Anisotropy of Dielectric Properties of Polymer Materials

18420188N Minsk VESTSI AKADEMII NAVUK BSSR: SERYYA FIZIKA-TEKNICHNYKH NAVUK in Russian No 1, Jan-Mar 89 (Manuscript received 10 Jan 88; deposited at VINITI 25 Apr 88) p 117

[Abstract of article by A. A. Dzhezhora, V. L. Shushkevich, Vitebsk Technological Institute of Light Industry]

[Text] The electric field and capacitance are calculated for a sensor used to study the anisotropy of dielectric properties of flat polymer materials. The field and capacitance of the sensor are analyzed where the thickness of the material is less than its geometric dimensions. Diagrams are presented of the anisotropy of dielectric permeability of several materials. References 5.

UDC 537.322.11:536.212+539.3

Calculation of Thermal Mode in Thermoelectric Measurements

18420188O Minsk VESTSI AKADEMII NAVUK BSSR: SERYYA FIZIKA-TEKNICHNYKH NAVUK in Russian No 1, Jan-Mar 89 (Manuscript received 19 Jan 88; deposited at VINITI 25 Feb 88) pp 117-118

[Abstract of article by A. A. Lukhvich, A. N. Zakharov, Institute of Applied Physics, Belorussian Academy of Sciences]

[Text] The thermal mode of a homogeneous, semilimited body is computed as a function of time, its heat-physical and elastic properties and the parameters of the thermoelectric converter. The equations produced allow calculation of the temperature and temperature gradient along the axis of a heated thermoelectrode both at the point of contact of the electrode with the body, and within the depth of the electrode. The equations can be used to perform practical calculations and to optimize methods and devices for thermoelectric monitoring. References 3.

UDC 681.51.015:519.876.5

Simulation Model and Algorithm for Estimating Probability Characteristics of Monotonic Structures

18420188P Minsk VESTSI AKADEMII NAVUK BSSR: SERYYA FIZIKA-TEKNICHNYKH NAVUK in Russian No 1, Jan-Mar 89 (Manuscript received 11 Oct 87; deposited at VINITI 25 Feb 88) p 118

[Abstract of article by A. A. Mkrtchyan, Institute of Technical Cybernetics, Belorussian Academy of Sciences]

[Text] A comparative analysis is presented of the most effective methods for estimating the probability characteristics of monotonic structures. It is shown that solution of this problem in the class of known analytic methods involves great computational difficulties. An algorithm is suggested for estimating the probability characteristics of monotonic structures of arbitrary type with heterogeneous probability characteristics of elements based on methods of simulation modeling. The promise of this approach and the possibility of decreasing computer time required to study structurally complex systems of many dimensions are demonstrated. References 11.

UDC 621.777

Formation of Briquettes of Aluminum-Based Powders

18420188Q Minsk VESTSI AKADEMII NAVUK BSSR: SERYYA FIZIKA-TEKNICHNYKH NAVUK in Russian No 1, Jan-Mar 89 (Manuscript received 8 Dec 87; deposited at VINITI 13 Jan 88) p 118

[Abstract of article by A. T. Volochko, A. P. Chelyshev, Deceased, I. N. Rumyantseva, Institute of Physics and Technology, Belorussian Academy of Sciences]

[Text] Results are presented from studies of pressing conditions of briquettes of aluminum powders with graphite particles.

The relationship between pressure and porosity is established. The basic regularities are established for pressing of a mixture of aluminum and graphite powders.

Results of the studies allow determination of the optimal parameters of the process, computation of the force necessary for production of quality briquettes of the required size with predetermined density. References 6.

UDC 681.325

Dynamic Priority Devices (A Review)

18420188R Minsk VESTSI AKADEMII NAVUK BSSR: SERYYA FIZIKA-TEKNICHNYKH NAVUK in Russian No 1, Jan-Mar 89 (Manuscript received 4 Dec 87; deposited at VINITI 13 Jan 88) p 119

[Abstract of article by V. Ye. Chernyavskiy, Institute of Technical Cybernetics, Belorussian Academy of Sciences]

[Text] A study is made of dynamic priority devices with explicit assignment of prioities of requests, intended for hardware solution of access conflicts to a single shared resource.

A dynamic priority device refers to a device with N channels, each channel having a request input R_i (i = 1, ..., N), a channel priority code input P_i and a permission output g_i. The function of the dynamic priority device is to select the group of channels with highest priority containing requests, i.e., to formulate the values of g_i such that:

$$g_i = \begin{cases} 1, & (r_i = 1) \wedge (P_i = \max\limits_j \{P_j \mid r_j = 1\}), \\ 0, & (r_i = 0) \vee (P_i \neq \max\limits_j \{P_j \mid r_j = 1\}), \end{cases}$$

where j = 1, ..., N.

The principles of structural and algorithmic organization of the dynamic priority device are determined, a classification of such devices is presented and the peculiarities characteristic of each class of dynamic priority device are determined. The work is illustrated by a large number of examples. References 31.

UDC 620.179.14

Experimental Studies of Sensitivity of Tubular Ferroprobes With Transverse Excitation

18420188S Minsk VESTSI AKADEMII NAVUK BSSR: SERYYA FIZIKA-TEKNICHNYKH NAVUK in Russian No 1, Jan-Mar 89 (Manuscript received 16 Sep 87; deposited at VINITI 13 Jan 88) p 119

[Abstract of article by B. P. Korennoy, N. N. Zatsepin, V. G. Gorbash, M. N. Delendik, Institute of Applied Physics, Belorussian Academy of Sciences]

[Text] Experimental studies are performed of the variation in mean differential sensitivity of thin-film tubular ferroprobes with transverse excitation as a function of frequency, excitation field strength and thickness of the active ferromagnetic rod coating. It is shown that there are optimal values of both frequency and excitation current for excitation of tubular ferroprobes, which depend on the thickness of the active core layer. References 3.

UDC 620.179.14

Influence of Electric Discharge on Electrochemical Properties of Tested Materials

18420188T Minsk VESTSI AKADEMII NAVUK BSSR: SERYYA FIZIKA-TEKNICHNYKH NAVUK in Russian No 1, Jan-Mar 89 (Manuscript received 20 Sep 87; deposited at VINITI 19 Dec 87) p 120

[Abstract of article by S. V. Dezhkunova, Institute of Applied Physics, Belorussian Academy of Sciences]

[Text] Results are presented from a combined study of changes in surface properties arising during testing of metal products by an electric discharge method.

The electrochemical properties and thermo-emf were studied, microstructural studies of specimens of St3, D16, Cu1, Ni, type 12Kh18N10T steel were performed on an electron microscope.

It is shown that the degree of action of the discharge on the surface depends on the test conditions. With exposure times of 0-70 s and discharge intervals, d, of approximately 0.1 mm, assuring generation of an image on the recording materials, no noticeable changes were observed on the surface such as changes in the structure or the nature of the potentiodynamic curves.

The degree of influence of the discharge increases with an increase in time or discharge gap. It follows from the results presented that when tests are performed in the field of an electric discharge, the possibility must be considered of irreversible changes in surface properties. References 4.

UDC 534.134

Designing Ultrasound Radiators by Electrodynamic Analogy Method

18420188U Minsk VESTSI AKADEMII NAVUK BSSR: SERYYA FIZIKA-TEKNICHNYKH NAVUK in Russian No 1, Jan-Mar 89 (Manuscript received 12 Mar 87; deposited at VINITI 11 Nov 87) p 120

[Abstract of article by N. V. Delenkovskiy, V. Ya. Pavlovskiy, Institute of Applied Physics, Belorussian Academy of Sciences]

[Text] A study is made of a method of designing ultrasound radiators using electrodynamic analogies and analog computers. A real oscillating circuit with distributed parameters is represented as discrete masses and rigid bars connected in series. Dynamic models of a conical ultrasonic concentrator and a cylindrical titanium waveguide with a niobium alloy lining are studied assuming that there is a temperature gradient along their length. The geometric parameters of the models are optimized. It is shown that a real oscillating system designed by this method has an oscillating amplitude 1.5-1.8 times greater than the system designed by the ordinary method which does not consider temperature gradients, at a temperature of 1200-1250°K. References 5.

UDC 638.652

Calculation of Phase Volumes in Elastically Deformed Ferromagnetics With BCC Structure

18420188V Minsk VESTSI AKADEMII NAVUK BSSR: SERYYA FIZIKA-TEKNICHNYKH NAVUK in Russian No 1, Jan-Mar 89 (Manuscript received 22 Dec 87; deposited at VINITI 13 Apr 88) p 121

[Abstract of article by Ye. M. Prikhodko, I. I. Branovitskiy, Institute of Applied Physics, Belorussian Academy of Science]

[Text] Based on the Akulov and Kondorskiy statistics, the volumes of magnetic phases are computed for an elastically deformed ferromagnetic with bcc structure, located in a magnetic field.

Magnetic phase distribution functions are obtained, allowing, in a number of practically important cases, consideration of existing methods for computing even effects and the magnetic state of ferromagnetics with bcc structure.

10

This is a U.S. Government publication. Its contents in no way represent the policies, views, or attitudes of the U.S. Government. Users of this publication may cite FBIS or JPRS provided they do so in a manner clearly identifying them as the secondary source.

Foreign Broadcast Information Service (FBIS) and Joint Publications Research Service (JPRS) publications contain political, economic, military, and sociological news, commentary, and other information, as well as scientific and technical data and reports. All information has been obtained from foreign radio and television broadcasts, news agency transmissions, newspapers, books, and periodicals. Items generally are processed from the first or best available source; it should not be inferred that they have been disseminated only in the medium, in the language, or to the area indicated. Items from foreign language sources are translated; those from English-language sources are transcribed, with personal and place names rendered in accordance with FBIS transliteration style.

Headlines, editorial reports, and material enclosed in brackets [ ] are supplied by FBIS/JPRS. Processing indicators such as [Text] or [Excerpts] in the first line of each item indicate how the information was processed from the original. Unfamiliar names rendered phonetically are enclosed in parentheses. Words or names preceded by a question mark and enclosed in parentheses were not clear from the original source but have been supplied as appropriate to the context. Other unattributed parenthetical notes within the body of an item originate with the source. Times within items are as given by the source. Passages in boldface or italics are as published.

SUBSCRIPTION/PROCUREMENT INFORMATION

The FBIS DAILY REPORT contains current news and information and is published Monday through Friday in eight volumes: China, East Europe, Soviet Union, East Asia, Near East & South Asia, Sub-Saharan Africa, Latin America, and West Europe. Supplements to the DAILY REPORTs may also be available periodically and will be distributed to regular DAILY REPORT subscribers. JPRS publications, which include approximately 50 regional, worldwide, and topical reports, generally contain less time-sensitive information and are published periodically.

Current DAILY REPORTs and JPRS publications are listed in *Government Reports Announcements* issued semimonthly by the National Technical Information Service (NTIS), 5285 Port Royal Road, Springfield, Virginia 22161 and the *Monthly Catalog of U.S. Government Publications* issued by the Superintendent of Documents, U.S. Government Printing Office, Washington, D.C. 20402.

The public may subscribe to either hardcover or microfiche versions of the DAILY REPORTs and JPRS publications through NTIS at the above address or by calling (703) 487-4630. Subscription rates will be provided by NTIS upon request. Subscriptions are available outside the United States from NTIS or appointed foreign dealers. New subscribers should expect a 30-day delay in receipt of the first issue.

U.S. Government offices may obtain subscriptions to the DAILY REPORTs or JPRS publications (hardcover or microfiche) at no charge through their sponsoring organizations. For additional information or assistance, call FBIS, (202) 338-6735,or write to P.O. Box 2604, Washington, D.C. 20013. Department of Defense consumers are required to submit requests through appropriate command validation channels to DIA, RTS-2C, Washington, D.C. 20301. (Telephone: (202) 373-3771, Autovon: 243-3771.)

Back issues or single copies of the DAILY REPORTs and JPRS publications are not available. Both the DAILY REPORTs and the JPRS publications are on file for public reference at the Library of Congress and at many Federal Depository Libraries. Reference copies may also be seen at many public and university libraries throughout the United States.